Summertime evaporation over two lakes in the Schirmacher Oasis~~oasis~~, East Antarctica

Elena Shevnina[1], Timo Vihma[1], Miguel Potes[2,~~3~~] and Tuomas Naakka[1]

[1] Finnish Meteorological Institute, Helsinki, 00560, Finland
~~[2] Institute of Earth Sciences (ICT), Institute for Advanced Studies and Research (IIFA), University of Évora, Évora, Portugal~~
[2] Universidade de Évora, Center for Sci-Tech Research in EArth sysTem and Energy (CREATE)~~[3] Earth Remote Sensing Laboratory (EaRSLab), Institute for Advanced Studies and Research (IIFA), University of Évora~~, Évora, 7002-554, Portugal

Correspondence to: Elena Shevnina (elena.shevnina@fmi.fi)

Abstract. Amount of liquid water has been continuously grown in coastal Antarctica. It accumulated in the hydrological system including rivers and lakes existing both on ice surface and inside it. This complex hydrological system is poorly understood and it is challenging without comprehensive measurements of components of hydrological balance. This study focused on lake evaporation which were measured directly on two lakes located in the Schirmacher Oasis (70 °S, Antarctica) with the eddy-covariance (EC) technique. The experiment lasted during two austral summers (December–February) in 2017–2018 and 2019–2020. The lakes were warmer than ambient air during whole summers, and they became ice free for the period of 3–6 weeks. The measurements showed that summertime evaporation varied from 0.3 to 5.0 mm d^{-1}, and depending on the ice cover presence, the average evaporation ranged from 1.5 ± 0.1 mm d^{-1} in December to 3.0 ± 0.2 mm d^{-1} in January–February. The EC measurements were used as a reference for evaluating uncertainties of five empirical formulas and bulk-aerodynamic method implementing various turbulent transfer coefficients. The bulk-aerodynamic method with locally adjusted turbulent transfer coefficients shows the most accurate estimates of daily rates of the lake evaporation (of 6–8 %). The empirical formulas underestimated the seasonal rate of lake evaporation by 27–73 %. Our results indicate that wind speed is the primary factor that controls summertime evaporation over the lakes. The largest day-to-day variations in evaporation were associated with changes in the wind speed.

~~**Abstract.** The evaporation over two glacial lakes in the Schirmacher Oasis (70 °S, Antarctica) was measured by the eddy-covariance (EC) technique during the austral summers (December – February) in 2017 – 2018 and 2019 – 2020. These direct measurements showed that summertime evaporation over two lakes varied from 0.3 to 5.0 mm d^{-1}. Depending on the ice cover presence, the average evaporation varied from 1.5 ± 0.1 mm d^{-1} in December to 3.0 ± 0.2 mm d^{-1} in January – February. In summer, both lakes were warmer than the ambient air, and the largest day-to-day variations in evaporation were associated with variations in the wind speed. The EC measurements were used as a reference for evaluating the uncertainties of the empirical formulas and bulk-aerodynamic method. The bulk-aerodynamic method shows the most accurate estimates of lake evaporation (of 6 – 8 %). The empirical formulas underestimated the evaporation by 27 – 73 %.~~

1 Introduction

The Antarctic coast hosts numerous water bodies that store meltwater within a complex hydrological system of lakes and rivers. Every summer, approximately 60,000 surface lakes form on ice shelves (Corr et al., 2022; Dirscherl et al., 2021); the largest, reaching up to 80 km in length, are found in East Antarctica (Shen et al., 2025; Stokes et al., 2019). The presence of these water bodies accelerates the marginal calving of ice sheets — contributing to global sea level rise — and increases the risk of hydrofracturing-induced collapse of ice shelves (Rignot et al., 2004; Banwell et al., 2013). Large lakes also influence local weather: by providing a moisture source to the atmosphere through evaporation, they warm the air, increase precipitation, and foster fog formation (Blanken et al., 2003; Gultepe et al., 2003; Rouse et al., 2005; Gilson et al., 2018; Su et al., 2020).

Antarctica hosts approximately 120 permanent settlements, most of which are located along the continental coast, in rock oases, or on sub-Antarctic islands (Antarctic station catalogue, 2025). These sites typically house between 20 and 80 people, primarily consisting of scientists, logistics personnel supporting fundamental research, and tourists. Antarctic tourism grew from about 6,500 visitors in the 1991–1992 season to nearly 105,000 in the 2022–2023 season. Post-pandemic, arrival numbers of tourists increased by 40% and are projected to grow by 12.5% annually (Bastmeijer et al., 2023). Nearby lakes provide a crucial freshwater supply for the settlements; consequently, evaluating water resources is essential for managers planning site maintenance and infrastructure investments, as well as for mitigating hydrological risks (Lan et al., 2025). Assessing these resources requires reliable hydrometeorological observations and robust hydrological models. Furthermore, Antarctic lakes shelter unique life forms that are sensitive to human intrusion and climate change (Rothschild and Mancinelli, 2004; Andersen et al., 2011; Keskitalo et al., 2013). Understanding the hydrological regimes of these lakes is therefore vital for the conservation of these ecosystems (Faucher et al., 2019).

Antarctica hosts numerous water bodies that store meltwater within a complex hydrological system of lakes and streams. Every summer, approximately 60,000 supraglacial lakes are formed on the ice shelf (Corr et al., 2022; Dirscherl et al., 2021), the largest lakes found in East Antarctica are up to 80 km long (Shen et al., 2025; Stokes et al., 2020). These lakes accelerate the marginal glacier calving (contributing to the global sea level rise), and increase risk of hydrofracture-induced collapse of ice shelves (Rignot et al., 2004; Banwell et al., 2013; Arthur et al., 2022). Providing a moisture source to the atmosphere through evaporation, lakes affect local weather by increasing the precipitation and fostering fog formation (Blanken et al., 2003; Gultepe et al., 2003; Rouse et al., 2005; Su et al., 2020).

Antarctica hosts approximately 120 permanent settlements in Antarctica, most of them located along the continental coast, in rock oases and sub-Antarctic islands (Antarctic station catalog, 2025). Since the COVID-19 pandemic, the number of people visiting Antarctica has increased by 40%, and is expected to grow further by approximately 12.5% per year (Bastmeijer et al., 2023). The nearest lakes provide a freshwater supply for the settlements, and evaluation of their water resources is a crucial task for their managers (Kaup, 2004; Sokratova, 2011). The managers plan on the maintenance and infrastructure investments based on assessment of freshwater resources and hydrological risks (Lan et al., 2025). This assessment requires

~~reliable hydrometeorological observations and robust models to evaluate hydrological stability. Furthermore, the Antarctic lakes house unique lifeforms (Rothschild and Mancinell, 2004; Andersen et al., 2011; Keskitalo et al., 2013). Understanding the lake hydrological regime is important to save these ecosystems (Faucher et al., 2019).~~

The lake water balance equation describes changes in ~~a~~ lake volume as the difference between inflow components (e.g., surface/subsurface~~of inflow (surface/underground~~ runoff, precipitation~~, etc~~) and outflow components (e.g., ~~components (~~evaporation/sublimation, artificial water withdrawal~~, surface/underground runoff, etc~~). Depending on the specific site~~case~~ and the integration timescale (e.g.,~~time scale—whether~~ daily, seasonal, decadal), ~~or decadal—~~the contribution of certain components may be negligible, while others remain essential~~ (Chebotarev, 1975)~~. Evaporation, in particular, is a critical~~crucial~~ component of the water balance for lakes in polar regions (Le et al., 2016; Leppäranta et al., 2020; Wang et al., 2020; Shi et al., 2024). However, because evaporation is difficult to measure directly, it is often estimated using indirect methods that require only limited hydrological and meteorological ~~hydrometeorological~~ observations (Morton, 1990; Finch and Hall, 2001; Spence et al., 2003).

A wide diversity of approaches exists to estimate lake evaporation indirectly from observations (Keijman, 1974; Spence and Hedstrom, 2015; ~~meteorological and hydrological observations (~~Spank et al., 2025). These methods can be categorized~~; Keijman, 1974). The indirect approaches are divided~~ into mass and energy balance models, bulk aerodynamic (mass-transfer) techniques, combination methods~~, combination~~, equilibrium temperature models,~~and~~ empirical formulas, and the use of evaporation pans or tracers such as ~~pans or sticks and tracers i.e.~~ water isotopes (Finch and Hall, 2001; Finch and Calver, 2008; Abtew and Melesse, 2013; Bellagamba et al., 2021). The use of evaporation pans is a traditional approach that can provide high accuracy when properly calibrated (Stanhill, 2002). Alternatively, in mass and energy ~~In the energy balance and mass (water)~~ balance approaches, ~~the~~ evaporation is typically estimated as the residual of the~~together with residuals of a~~ balance equation, provided all other components are known and accurately quantified (Singh and Xu, 1997; Stannard and Rosenberry, 1991; Abtew and Melesse, 2013).

The bulk-aerodynamic approach estimates evaporation based on data regarding ~~estimated the evaporation on the basis of data on a~~ land surface properties (type, temperature, and ~~whether a land surface type is an ice or a lake or rock or a forest, surface temperature and surface~~ roughness) and atmospheric variables (wind speed, specific humidity, and air temperature) within~~in~~ the lowermost ~~part of the~~ atmospheric boundary layer (Brutsaert, 1982). This method requires ~~It needs~~ meteorological observations at ~~on the~~ different levels above the surface ~~land surface allowing it~~ to calculate ~~heat fluxes (~~sensible and latent heat fluxes ~~)~~ from their gradients. Evaporation is then derived by dividing the ~~The~~ latent heat flux ~~divided~~ by the latent heat of vaporization~~ yields evaporation~~. The bulk aerodynamic approach employs ~~the~~ transfer coefficients for ~~(~~turbulence, heat, and moisture, which are ~~)~~ derived from flux-gradient relationships and semi-empirical profiles for wind, temperature, and humidity (Yang and Bai, 2023). Under specific conditions, this method~~; in particular situations, it~~ adequately estimates ~~the~~ surface evaporation on daily or shorter timescales (Moore, 1983). This ~~Consequently, this~~ method has been widely applied to assess evaporation and sublimation over lakes and glaciers in Antarctica (Clow et al., 1988; Bliss et al., 2011; Leppäranta et al., 2016).

Combination approaches integrate elements of both the energy budget and mass-transfer principles (Penman, 1948). A more comprehensive form is the Penman-Monteith equation (Monteith, 1965), which was originally developed to estimate~~describe~~ evapotranspiration from vegetated surfaces. ~~vegetation.~~ In the empirical approach, daily or~~and~~ monthly lake evaporation rates are related to~~rate is correlated with~~ variables such as lake surface area, incoming solar radiation, diurnal minimum and maximum of air temperature and relative humidity (Konstantinov, 1968, Zhao et al., 2013, Spank et al., 2025). Simplified versions of both~~the~~ combination and empirical formulas have been applied to Antarctic lakes although their associated ~~Antarctica lakes even though their~~ uncertainties are not well known ~~unknown~~ (Borghini et al., 2013; ~~Shevnina and Kourzeneva, 2017;~~ Dhote et al., 2021; Kuznetsova et al., 2021). A key limitation ~~The disadvantage~~ of the empirical, mass transfer and combination approaches is that their performance is restricted to the geographical and climatic conditions, under which ~~the specific geographical locations where~~ their empirical coefficients were originally derived (Finch and Hall, 2001). To improve their applicability~~overcome this~~, the mass transfer coefficients are often calibrated based on measurements from eddy covariance (EC) systems (Ala-Könni et al., 2022, Nordbo et al. 2011). What is unknown is the actual range of values of the transfer coefficients for Antarctica, this study quantify them.~~in Antarctica.~~

In this study, we evaluated summertime~~This study evaluated the~~ evaporation over two lakes in the Schirmacher Oasis (East Antarctica), using both the direct observations and various ~~, East Antarctica from direct eddy-covariance method and~~ indirect mass-transfer methods~~method and empirical formulas~~. The study quantified~~quantifies~~ the uncertainties of five empirical formulas~~equations~~ and bulk-aerodynamic method by comparing them against ~~formulae against the~~ eddy-covariance measurements collected during the ~~measurement collected on two lakes in in two~~ austral summers of~~in~~ 2017–2018 and 2019–2020.

2 Study area

The Schirmacher Oasis (70°45′ S, 11°38′ E) is situated approximately 80 km from the coast of the Lazarev Sea, Dronning Maud Land (Fig. 1a). This oasis is an ice-free rock outcrop, approximately 20 km long and 3 km wide, elongated in a west-northwest to east-northeast direction (Simonov and Fedotov, 1964). The relief consists of rocky hills with elevations reaching up to 228 m above sea level (asl.), primarily composed of gneiss mixed with basalt (Sengupta, 1991). Discovered in 1939, the site saw its first settlements emerge in the late 1960s. Today, the oasis hosts two year-round scientific observatories and two seasonally occupied tourist camps (Fig. 1b). The observatories are staffed by 15–25 overwintering personnel, with up to 30 additional staff visiting during the summer. The two tourist camps accommodate up to 20 people each and operate from November to February. Two ice runways support the transport of personnel and cargo; fuel and supplies are primarily delivered by ship to coastal bases on the ice shelf and subsequently transported to the settlements by vehicles. These settlements, ice runways, and coastal bases are connected by year-round ice roads (indicated by yellow lines in Fig. 1b). During the summer, transportation along these routes is often hindered by meltwater lakes and streams that form on the ice (Fig. 1c).

The Schirmacher oasis (70°45′ S, 11°38′ E) is situated approximately 80 km from the coast of Lazarev Sea, Dronning Maud Land (SA, Fig. 1 a). The oasis is an ice-free rock outcrop approximately 20 km long and 3 km wide (Fig. 1 a), elongated in the west–northwest to east–north-east direction (Simonov and Fedotov, 1964). The relief is hillrocks with absolute heights up to 228 m above sea level (asl). The rock hills mostly consist of gneiss mixed with basalts (Sengupta, 1991). The Oasis was discovered in 1939, and first settlements emerged primarily for science in the late 1960s. Now, the oasis now shelters two scientific observatories operated year round and two tourist camps occupied seasonally (Fig. 1b). The observatories are crewed by 25–30 overwintering personnel, and up to 50 personnel are visiting the site during summers. Two tourist camps accommodated up to 20 people, and operated from November to February. Two ice runways support transportation of people and cargo. Fuel and goods are mostly delivered by ships to coastal bases located on the ice shelf, and then transported to the settlements by vehicles. The settlements, ice runways and coastal bases are connected with year-round ice roads (yellow lines in Fig. 1 b). In summertime, the transportation along the ice roads is hindered by meltwater lakes and streams formed over the ice. Figure 1 c shows the melted ice road to the White Desert Camp in December 2019.

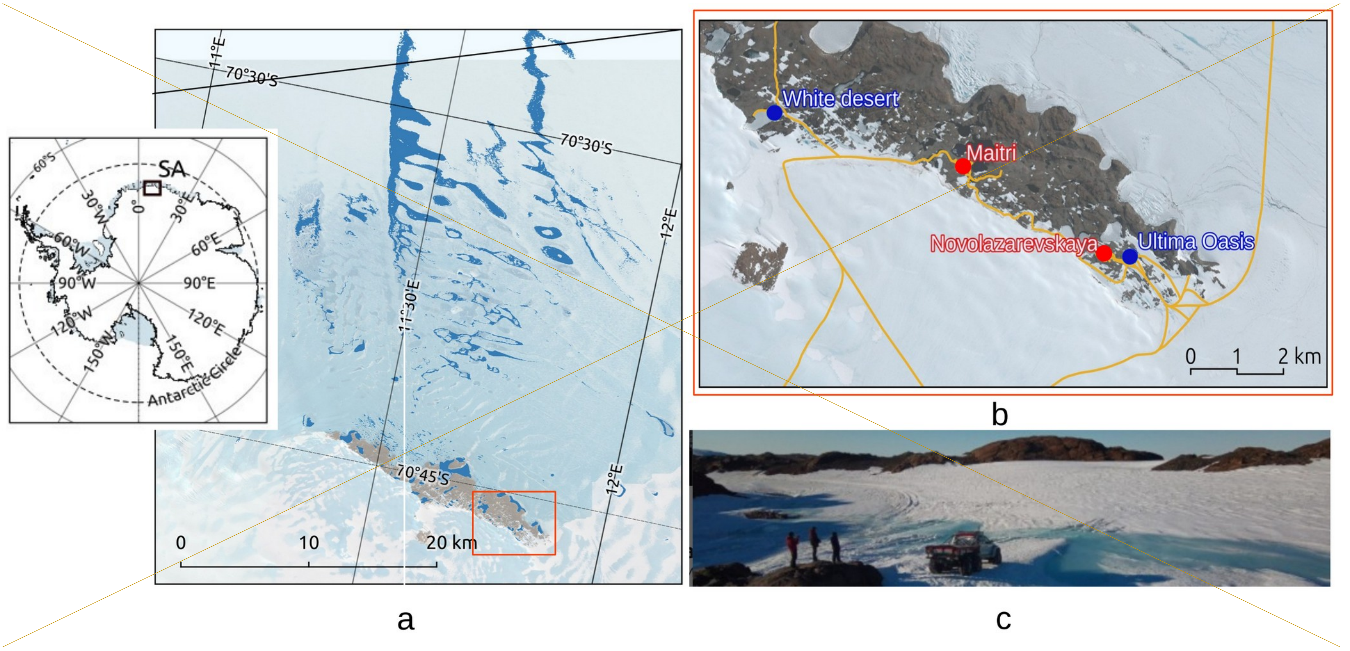

a b c

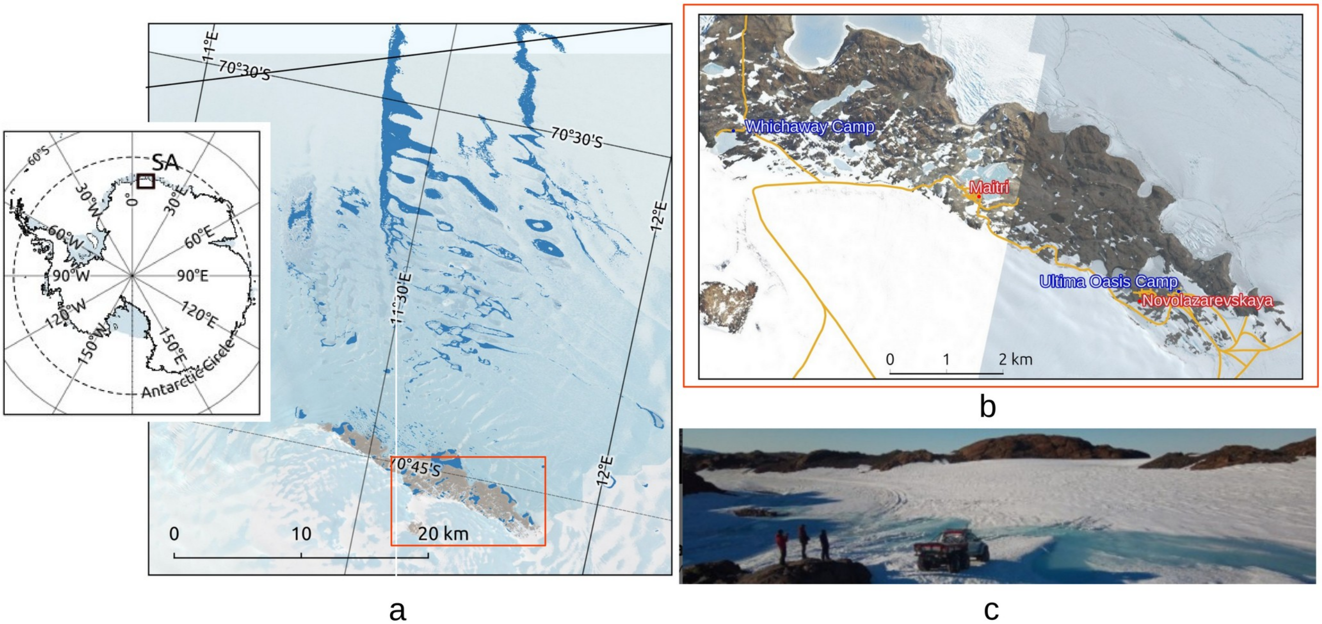

Figure 1:Fig. 1. Location of the Schirmacher oasis (SA) (a) and its social infrastructure (b): year round (red dots) and seasonal (blue dots) settlements connected by roads (yellow lines, © Humanitarian OpenStreetMap Team (HOT), 2020. Distributed under the Open Data Commons Open Database License ((ODbL) v1.0.). © Google Maps, 2019. The red boxes in (a) and (b) outline the area with the main infrastructure in SA, and the image (c) shows the a flooded section of the melted ice road leading to the WhichawayWhite Desert Camp (photo by D. Emelyanov, December 2019).

Lakes have existed in the Schirmacher Oasis since the Late Quaternary (Phartiyal et al., 2011), and today, the oasis is home to approximately 300 lakes (Gerrish et al., 2008). Most of these are freshwater bodies nourished by ice melt and seasonal snow cover, remaining ice-free for 6–12 weeks during the summer (Simonov, 1971). The largest lakes are glacial — directly attached to the ice sheet — and are often connected by temporary streams, forming chains that terminate in epishelf saline lakes (Loopman et al., 1988). Landlocked lakes, which have no connection to the ice sheet, are fed solely by snow melt and may evaporate over time, eventually forming hollows or dry beds (Fedorova et al., 2011). This study focuses on two glacial lakes that differ in volume and depth, both of which become ice-free for 2–8 weeks during almost every summer season (Khare et al., 2008; Sharov and Tolstikov, 2018).

Lake Zub (also known as Lake Priyadarshini) is the second-largest lake in the oasis, with a volume of $1.02 \cdot 10^6$ m^3. Its maximum depth is 6.0 m (mean depth: 2.9 m), and it has a surface area of $35 \cdot 10^3$ m^2 (Dhote et al., 2021). During the 2017–2018 austral summer, the lake was ice-free from late December 2017 to early February 2018. Lake Zub/ Priyadarshini was reported to be thermally homogeneous during the period spanning from mid-January 1996 to mid-February 1997 (Sinha and Chatterjee, 2000). Lake Glubokoe is the deepest lake in the oasis, with a maximum depth of 34.5 m (mean depth: 13.1 m), a surface area of $147 \cdot 10^3$ m^2 , and a volume of $1.93 \cdot 10^6$ m^3 (Loopman et al., 1988). Until the late 1990s, it remained ice-covered year-round (Kaup, 2005).

The climate of the Schirmacher Oasis is characterized by low air humidity and temperatures; persistent katabatic winds that occur throughout most of the year. Two scientific observatories operate within the oasis (Fig. 1a): the Novolazarevskaya (Novo) observatory (70° 46′ 36″S, 11° 49′ 21″E), which began observations in 1961, and the Maitri observatory (70° 46′ 00″S, 11°43′ 53″E), which has been operational since 1989. These stations are situated approximately 5.5 km apart, and their meteorological measurements follow standards of the World Meteorological Organization (Turner and Pendlebury, 2004). Table 1 presents the monthly air temperature and relative humidity, averaged over the 1961–2010 period, based on observations from the Novo site (available at: http://www.aari.aq/default_ru.html, last accessed 7 December 2021).

Lakes have existed since the Late Quaternary in the Schirmacher Oasis (Phartiyal et al., 2011), and today, the oasis is home to approximately 300 lakes (Gerrish et al., 2008). Most of these are freshwater waterbodies, nourished by ice melt and seasonal snow cover, and remain ice-free for 6 – 12 weeks in summer (Simonov, 1971). The largest lakes are attached to the ice sheet (glacial), and are connected by temporary streams into chains that end up in epishelf saline lakes (Loopman et al., 1988). Lakes with no connection to ice are landlocked: they are fed by only snow melt, and evaporate through time forming hollows and dry beds (Fedorova et al., 2011). This study focuses on two lakes differing in volume and depth, and both becoming ice free almost every summer for 2–8 weeks (Khare et al., 2008; Tolstikov et al., 2018).

Lake Zub/Priyadarshini is the second largest lake in the Oasis with a volume of 1.02 $x10^6$ m^3. Its maximum depth is 6.0 m (mean depth is 2.9 m), and a surface area of 35,000 m^2 (Dhote et al., 2021). The lake was ice free from 29–31 December 2017 to 8–12 February 2018. Lake Zub/Priyadarshini was reported to be thermally homogeneous during the period spanning from mid-January 1996 to mid-February 1997 (Sinha and Chatterjee, 2000). Lake Glubokoe is the deepest lake in the Oasis with a maximum depth of 34.5 m (mean of depth is 13.1 m), a surface area of 147,000 m^2, and a volume of over 1.93 $x10^6$ m^3 (Loopman et al., 1988). Until the late 1990s, it was ice-covered year round (Kaup, 2005). This lake was free of the ice from 26 – 28 January 2019 to 23 – 25 February 2020.

The climate of the Schirmacher Oasis is characterized by low air humidity and temperature, and persistent (katabatic) wind blowing most of the year. There are two scientific observatories operating in the Schirmacher oasis (Fig. 1 a): Novolazarevskaya (Novo) observatory (70° 46′36″S, 11° 49′21″ E) starts the observations in 1961, and Maitri observatory (70° 46′00″S, 11° 43′53″ E) operates since 1989. They are located at a distance approx. 5.5 km, their meteorological measurements following the WMO's standards (Turner and Pendlebury 2004). Table 1 shows the monthly air temperature, relative humidity, averaged over the period of 1961–2010 according to the observations at Novo site (the data given by the Arctic and Antarctic Research Institute at http://www.aari.aq/default_ru.html, last access 07.12.2021).

Table 1. The monthly minimum, mean and maximum values for the meteorological parameters calculated from the measurements for the period of 1961–2010 (the values are separated by a slash).

Meteorological parameter	1961–2010		
	December	January	February
Air temperature, °C	–3.9 / –1.0 /1.5	–2.5 / –0.4 / 1.4	–4.7 / –3.3 / –1.0

Relative Humidity,%	47 / 56 / 69	49 / 56 /66	41 / 49 / 59
Atmospheric pressure, Pa	965 / 975 / 991	964 / 976 / 986	964/ 973 / 987
Wind speed, m s^{-1}	4.3 / 7.4 / 10.3	3.1 / 7.0 / 10.4	5.8 / 9.4 / 13.1
Soil surface temperature, ºC	3.0 / 6.7 / 10.0	3.0 / 6.7 /11.0	–2.0 / 0.2 / 4.0
Precipitation, mm	0.0 / 5.3 / 54.8	0.0 / 2.6 / 38.0	0.0 / 2.9 / 25.9

The study region is characterized by persistent katabatic winds blowing from the continental interior (Bormann and Fritzsche, 1995). To accurately capture eddy-flux measurements, it is essential to settle the instrumentation relative to the prevailing wind directions (Burba, 2013). Figure 2 illustrates wind directions and wind speed anomalies for December and January (1998–2016), calculated from 6-hourly synoptic observations at the Novo site, obtained from the British Antarctic Survey dataset (https://www.bas.ac.uk, last accessed 14 December 2018). Prevailing winds range from 110° to 140° (indicated by black arrows in Fig. 2), consistent with the expected direction of katabatic flow. Wind speed anomalies were estimated for 10-degree directional bins and are represented by the colour-coded legend in Figure 2. Positive wind speed anomalies are frequently observed within the prevailing wind range (indicated by orange, yellow, red, brown, and black colours in the legend); consequently, one can expect the majority of high-wind events to originate from these directions. However, the wind from the prevailing directions are not guaranteed to be of purely katabatic origin, as some may be driven by a combination of katabatic and synoptic forcing.

Meteorological parameter	1961 – 2010		
	December	January	February
Air temperature, °C	–3.9 / –1.0 /1.5	–2.5 / –0.4 / 1.4	–4.7 / –3.3 / –1.0
Relative Humidity,%	47 / 56 / 69	49 / 56 /66	41 / 49 / 59
Atmospheric pressure, Pa	965 / 975 / 991	964 / 976 / 986	964/ 973 / 987
Wind speed, ms^{-1}	4.3 / 7.4 / 10.3	3.1 / 7.0 / 10.4	5.8 / 9.4 / 13.1
Soil surface temperature, ºC	3.0 / 6.7 / 10.0	3.0 / 6.7 /11.0	–2.0 / 0.2 / 4.0
Precipitation, mm	0.0 / 5.3 / 54.8	0.0 / 2.6 / 38.0	0.0 / 2.9 / 25.9

The region of the study is featured with the persistent katabatic winds blowing from the continental interior (Bormann and Fritzsche, 1995). To represent an area covering eddy-flux measurements, it is important to place an instrumentation toward prevailing wind directions (Burba, 2013). Fig. 2 shows the wind directions and wind speed anomalies for December and January for the period 1998–2016 calculated from the 6-hour synoptic observations at the Novo site available from the British Antarctic Survey Dataset (https://www.bas.ac.uk, last accessed 14.12.2018). The prevailing wind directions range from 110 to 140º (marked with the black arrows in Fig. 2), and these winds come from a direction that would be the direction

~~of katabatic winds. However, it is not guaranteed that all these winds are entirely of katabatic origin, and some winds may be driven by a combined effect of katabatic and synoptic forcing. The wind speed anomalies were estimated for each 10 degree range in the wind direction, and they are given with the different colors in the legend to Fig. 2. The positive wind speed anomalies are often observed within the range of the prevailing wind directions (marked with orange, yellow, red, brown and black in the legend of Fig. 2). Therefore one can expect the majority of strong winds from these directions.~~

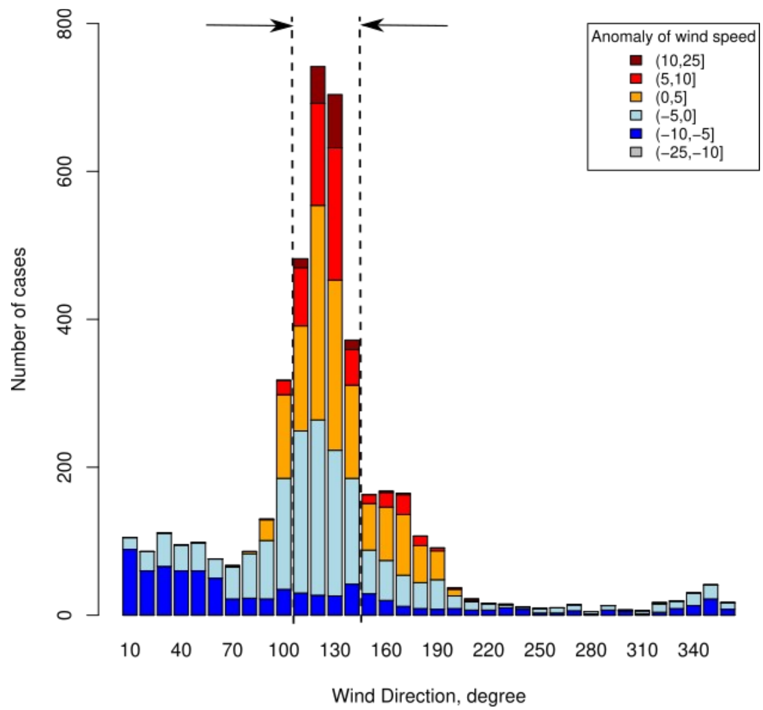

Figure 2:~~Fig. 2:~~ Wind direction and wind speed anomalies for ~~two austral summer months (~~December and January (1961–2010).

3 Data and methods

3.1 Micrometeological and hydrological observations

Measurements were collected on two lakes (Fig. 3a) across two separate field campaigns, covering 38 days in 2017–2018 and 33 days in 2019–2020. In the first experiment at Lake Zub /Priyadarshini, evaporation was measured while the lake was ice-free. The second experiment, conducted at Lake Glubokoe, captured the period of lake ice break-up. Although this experiment was originally designed to cover the entire austral summer, it was prematurely terminated in mid-January due to instrumentation failure.

~~The measurements were collected on two lakes (Fig. 3 a) in two different experiments covering 38 days in 2018 and 33 days in 2019 – 2020. In the first experiment on Lake Zub/Priyadarshini, the evaporation was measured during the period when the lake was free of ice. The second experiment on Lake Glubokoe covers the period of lake ice break-up; the experiment,~~

however, was planned to cover the whole austral summer but was terminated due to the instrumentation failure in mid-January.

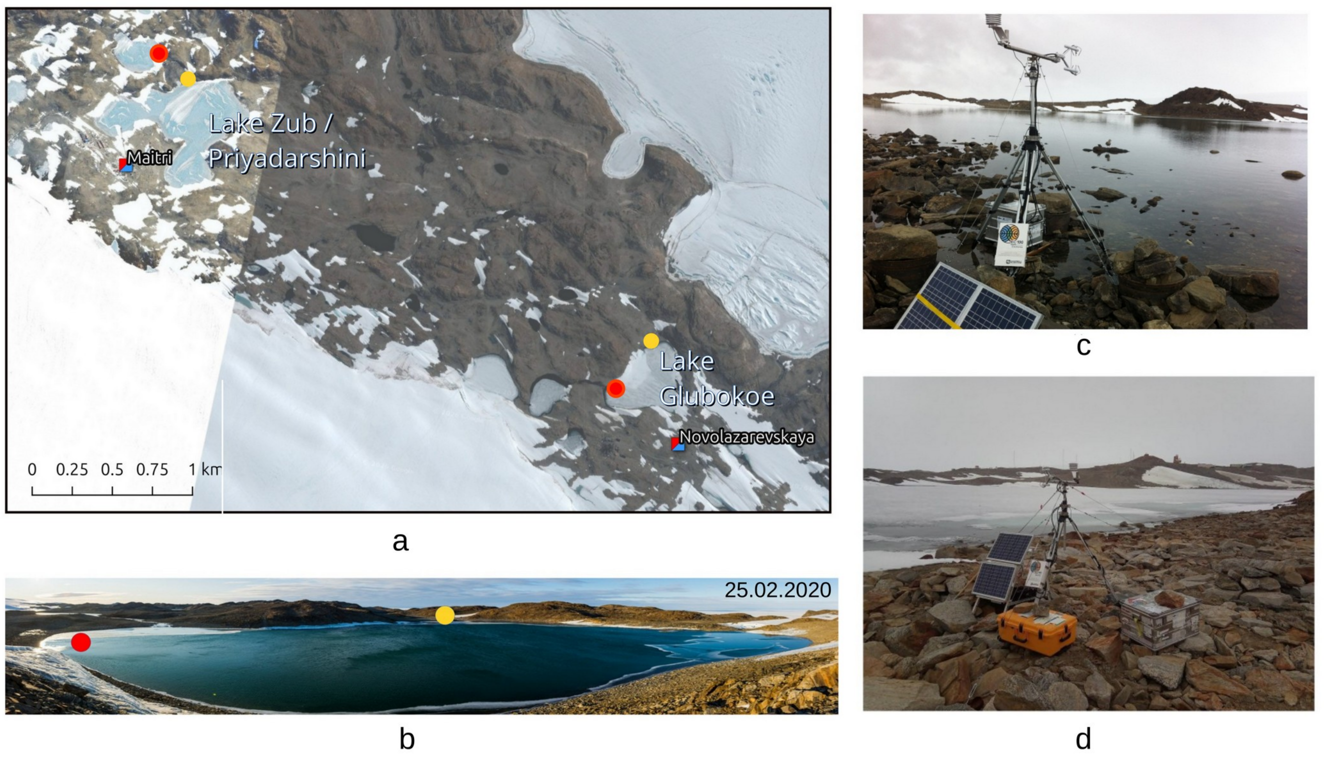

FigureFig. 3: Location of the instrumentation on the shores of two lakes (a): temperature and water level logger (red dots), the EC system (yellow dots), and digital cameras collecting the panoramic images (rounded red crosses), © Google Maps 2019. The photo (b) shows the location of the instrumentations installed on Lake Glubokoe (on the panoramic image from 25 February 2020). The photos on (c) and (d) show the EC system installed on the shore of Lake Zub/Priyadarshini (6 January 2018) and Lake Glubokoe (12 December 2019).

Air temperature, atmospheric pressure, wind speed and direction, water vapor concentration and relative humidity were measured using an IRGASON open-path EC system (Campbell Scientific). The instrument integrates a 3D sonic anemometer and gas analyser that measure CO_2/H_2O concentrations on a high frequency (10 Hz). The system was positioned 5–6 m from the lake shoreline and oriented toward the lake to align with prevailing wind directions. Lake surface water temperature (LSWT) was measured using HOBO sensors (indicated by red dots in Fig. 3a) installed at a depth of 0.02 m. Prior to installation, we conducted a 1–2 day inter-calibration of our sensors against the sensors installed at Novo observatory (data not shown).

The air temperature, atmospheric pressure, wind speed/direction and water vapour concentration were measured on a tower equipped with the EC open-path system IRGASON by Campbell Scientific. The instrument consists of a 3D sonic anemometer and two gas analysers measuring CO_2/H_2O concentrations on a high frequency (10 Hz). It was placed 5–6 m from the lake shoreline and oriented toward the lake in the direction of the prevailing winds. The lake surface water temperature (LSWT) was measured by the HOBO instrumentation (red dots in Fig. 3 a) installed at a depth of 0.02 m. We used the meteorological measurements from the Novo automatic weather station for a 1–2 day intercalibration with our sensors before their installation (data not shown).

3.2 Methods

3.2.1 Eddy-covariance measurements

The eddy-covariance (EC) technique was used to measure evaporation from the two study lakes. Raw measurements were processed with the EasyFlux software provided by the instrument manufacturer, and then post-processed following the method described by Potes et al. (2017). We also included screening to remove spikes (Vickers and Mahrt, 1997); the frequency of these spikes was recorded for quality control purposes. Although the EC instrumentation collects gas concentration data across the full 0–360° range, only data associated with the footprint over the lake surface were utilized. These measurements were filtered using the footprint model defined by Kljun et al. (2004). The quality-controlled and filtered measurements cover more than 80% of raw data. Furthermore, air relative humidity and the saturation vapour pressure deficit—defined as the difference between air and water temperatures—were calculated following Hoeltgebaum et al. (2020) and Stull (2017), respectively.

The EC technique (Burba, 2013) was used to measure evaporation from the two lakes. The raw measurements were post-processed following Potes et al. (2017). The data were processed to remove spikes (Vickers and Mahrt, 1997), and the spikes detected were counted for quality control. The EC instrumentation collects the gas concentration in 0–360° wind directions, but the only data collected from a sector associated with the footprint over the lake was accounted for. The measurements were filtered by the footprints defined according to Kljun et al. (2004). The air relative humidity and saturation vapor pressure deficit (corresponding to the difference between air and water temperatures) were calculated following Hoeltgebaum et al. (2020) and (Stull, 2017), respectively.

3.2.2 Empirical formulas

The general form of the formulas reads as $E = K\, w_z\, (e_s - e_z)$, where E is the evaporation (mm period^{-1}), w_z is the wind speed (m s^{-1}), $(e_s - e_z)$ is the water vapourvapor deficit (kPa), z refers to height (m), and K is an empirical function approximated with a small number of coefficients. In this study, we evaluated evaporation over two lakes with the formulas originally derived for tropical, temperate and cold climate regions (Table 2).

Table 2. The empirical equations applied to evaluate the lake evaporation.

Author(s) (year)	Formula	Climate : Köppen climate classification
Penman (1948), as given in Tanny et al. (2008)	$E = 0.26(1 + 0.54\, w_2)(e_s - e_2)$	Temperate
Doorenbos and Pruitt (1975)	$E = 0.26(1 + 0.86\, w_2)(e_s - e_2)$	Temperate
Odrova (1979)	$E = 0.14(1 + 0.72 w_2)(e_s - e_2)$	Cold
Shuttleworth (1993)	$E = 2.909\, A^{-0.05} w_2 (e_s - e_2)$	Tropical

Author(s) (year)	Formula	Climate : Köppen climate classification
Penman (1948), as given in Tanny et al. (2008)	$E = 0.26(1 + 0.54\, w_2)(e_s - e_2)$	Temperate
Doorenbos and Pruitt (1975)	$E = 0.26(1 + 0.86\, w_2)(e_s - e_2)$	Temperate
Odrova (1979)	$E = 0.14(1 + 0.72 w_2)(e_s - e_2)$	Cold
Shuttleworth (1993)	$E = 2.909\, A^{-0.05} w_2 (e_s - e_2)$	Tropical

In these formulas, E is evaporation (mm d^{-1}), w_2 is the wind speed at 2 m height (m sms^{-1}), and A is a lake surface area (m^2). We also verified against the independent observations the formula $E = -0.33(1 - 1.82 w_2)(e_s - e_2)$ suggested in Shevnina et al. (2022).

3.2.2 Bulk-aerodynamic method

Evaporation is defined as the vertical surface flux of water vapourvapor due to atmospheric turbulent transport. Lake evaporation is estimated from measurements of a lake water surface temperature, and relevant bulk properties of the air (Venäläinen et al., 1998; Brutsaert, 1982). We calculated the evaporation (kg m^{-2} s^{-1}) after the bulk-aerodynamic methods as follows:

$$E = \rho C_{Ez} \left(q_s - q_{az} \right) w_z \quad (1)$$

where, ρ is the air density (kg m^3); C_E is the turbulent transfer coefficient for moisture (Dalton number) at height z; q_s is the saturation specific humidity corresponding to the lake surface water temperature, q_{az} is the air specific humidity at height z, and w_z is the wind speed at height z. The turbulent transfer coefficient (C_{Ez}) depends on surface roughness and atmospheric stability, which we determined using both field measurements (eddy covariance and gradient) and values reported in the literature. For literature-based estimates, we utilized a value of C_E = 0.00107, as suggested by Heikinheimo et al. (1999) for boreal lakes. This value allows for a more accurate representation of the turbulent mixing regime over small lakes compared to marine environments (Sahlee et al., 2014).

~~where, E is the evaporation (kg m^{-2} s^{-1}); is the air density (kg m^{3}), C_E is the turbulent transfer coefficient for moisture (Dalton number), q_s is the saturation specific humidity corresponding to the lake surface temperature, q_z is the air specific humidity, and w_z is the wind speed. The subscript z refers to the observation height. The actual values for the turbulent transfer coefficient of moisture for a reference level z (C_{EZ}) depend on the surface roughness and atmospheric stratification. The dependence is determined either from field experiments (eddy covariance, gradient measurements and radiation) or from values reported in the literature; both methods were applied in this study. From the literature, the C_E was taken as 0.00107 following Heikinheimo et al. (1999) and Venäläinen et al. (1998), who suggested the value based on measurements over a boreal lake. It allows us to better take into account the different regime of turbulent mixing over a small lake compared to the sea (Sahlee et al., 2014).~~

Since the atmospheric surface-layer ~~stratification~~ is not always neutral, the stability~~stratification~~ effects on the turbulent transfer coefficient C_{EZ} were taken into account as follows:

$$C_{Ez}=\frac{C_{DzN}^{1/2}\,C_{EzN}^{1/2}}{\left[1-\left(\frac{C_{DzN}^{1/2}}{k}\right)\psi_m\left(\frac{z}{L}\right)\right]\left[1-\left(\frac{C_{EzN}^{1/2}}{k}\right)\psi_q\left(\frac{z}{L}\right)\right]} \qquad (2)$$

where C_{DzN}~~C_{DzN}~~ is the drag coefficient for a lake surface (unitless), k is the von Karman constant (0.4), ψ_m and ψ_q are the stability functions for momentum and moisture, respectively, and L is the Obukhov length (metre) (Obukhov, 1946). The subscript N in Eq. (2) refers to the neutral values of the transfer coefficients. The Obukhov length was used to adjust~~(Obukhov, 1946) allows adjusting~~ the transfer coefficients (C_D and C_E~~C_{Dz} and C_{Ez}~~) to account for atmospheric stability ~~actual stratification~~ in the ~~atmospheric~~ surface layer. For~~In~~ our calculations, the value of ~~neutral~~ drag coefficient (C_{DzN}) was set to 0.00181, following ~~C_{DN}) equals 0.00181 as suggested by~~ Heikinheimo et al. (1999). As these values were originally referenced to ~~The values by Heikinheimo et al. (1999) were given for~~ z = 3 m, we adjusted them ~~metres, and converted~~ to our observation heights (z = 2 m and z = ~~height (of 2 and~~ 1.8 m~~metres~~) using the approach proposed by Launiainen and Vihma (1990). This ~~, and the~~ same algorithm was applied to iteratively solve the interdependency between ~~of the~~ turbulent fluxes and the Obukhov length. Stability functions were defined using ~~For the stability functions, we used~~ the classic formulation~~form~~ by Businger et al. (1971) for unstable stratification and by ~~, and that of~~ Holtslag and de Bruin (1988) for stable stratification. Furthermore, ~~The actual values for~~ the turbulent transfer coefficient (C_E) and the drag coefficient (C_D) were adjusted from the EC measurements. Specifically, a wind-dependent C_E was derived from ~~also defined on the basis of the eddy covariance measurements. The wind dependent value for the C_E was defined on the basis of the~~ EC measurements at Lake ~~on~~ Zub/Priyadarshini during the 2017–2018 season and subsequently applied to calculate ~~(2017 – 2018), and applied in the calculation of~~ evaporation using Eq. (1) for ~~from the~~ independent observations collected at~~on~~ Lake Glubokoe (2019–2020). ~~– 2020).~~

The drag coefficient (C_{Dz}) and the moisture ~~C_{Dz} and~~ transfer coefficient (C_{Ez}) were also estimated based on ~~on the basis of the~~ EC measurements from~~on~~ Lake Glubokoe (2019–~~ – ~~2020) and subsequently applied to calculate ~~the~~ evaporation from observations atthe observations on Lake Zub/Priyadarshini (2017–—2018). Following Arya (1988), the coefficients were calculated as follows:

$$C_{Dz} = \frac{k^2}{\left[\ln\left(\frac{z}{z_{0m}}\right) * \Psi_m\left(\frac{z}{L}\right)\right]^2}. \tag{3}$$

$$C_{Ez} = \frac{k^2}{\left[\ln\left(\frac{z}{z_{0m}}\right) * \Psi_m\left(\frac{z}{L}\right)\right] * \left[\ln\left(\frac{z}{z_{0q}}\right) * \Psi_q\left(\frac{z}{L}\right)\right]}. \tag{4}$$

where z_{0m} is the momentum roughness length (metre)[m] and z_{0q} is the roughness length for water vapour (metre), according Fedorovich[m] according Ferdorovich et al. (1991):

$$z_{0m} = \frac{0.135\, v_a}{u_*} \; ; u_* \leq 10.856\left(\frac{cm}{s}\right), \tag{5}$$

$$z_{0m} = \frac{{u_*}^2}{69\, g} \; ; u_* > 10.856\left(\frac{cm}{s}\right), \tag{6}$$

$$z_{0q} = \frac{9.072 \times 10^{-2}}{u_*} \; ; u_* \leq 10.856\left(\frac{cm}{s}\right), \tag{7}$$

$$z_{0q} = 8.357 \times 10^{-3} - 1.904 \times 10^{-4}\left(u_* - 10.856\right) \; ; 10.856 < u_* < 22.622\left(\frac{cm}{s}\right), \tag{8}$$

$$z_{0q} = 1.092 \times 10^{-4}\, {u_*}^2 e^{-0.228 {u_*}^{3/4}} \; ; u_* > 10.856\left(\frac{cm}{s}\right). \tag{9}$$

where u_* is the friction velocity (m s^{-1}). The stability functions ψ_m and ψ_q assume the following forms:

$$\Psi_m\left(\frac{z}{L}\right) = \ln\left[\left(\frac{1+x^2}{2}\right)\left(\frac{1+x}{2}\right)^2\right] - 2\tan^{-1} x + \frac{\pi}{2} \text{ for } \left(\frac{z}{L} < 0\right), \tag{10}$$

$$\Psi_q\left(\frac{z}{L}\right) = 2\ln\left(\frac{1+x^2}{2}\right) \text{ for for } \left(\frac{z}{L} < 0\right), \tag{11}$$

$$\Psi_m\left(\frac{z}{L}\right) = \Psi_q\left(\frac{z}{L}\right) = -5\left(\frac{z}{L}\right) \text{ for for } \left(\frac{z}{L} \geq 0\right), \tag{12}$$

where $x = \left[1 - 16\left(\frac{z}{L}\right)\right]^{\frac{1}{4}}$. The value of the transfer coefficient of moisture (C_E) was further referred to Arya 1988.

Also, we also estimated the transfer coefficient of moisture as suggested in Andreas (1986):

$$C_{Dz}=\frac{k^2}{\ln\left(r/z_0\right)}, \tag{13}$$

$$C_{Ez}=\frac{\alpha_E k C_{Dz}^{1/2}}{k C_{Dz}^{-1/2}-\ln\left(z_Q/z_0\right)}, \tag{14}$$

where, the values of the z_Q and z_0 -were taken as the functions of the roughness Reynolds number, and were depended on the wind speed and on the surface roughness parameter; r is a reference heigh (10 metre); and α_E=1.

The estimated uncertainties of the indirect methods rely on the eddy-covariance (EC) technique (Tanny et al., 2008; Tran et al., 2023; Shi et al., 2024). To evaluate the skill of the indirect methods we apply the root mean square error ($RMSE$ = $\sqrt{\sum_1^n\left(E_{EC}-E_{mod}\right)^2}$) following Moriasi et al. (2007). –To define if a method is acceptable to be used in hydrological practice or not, we applied the s/σ criteria following to Popov (1979). In s/σ -criteria, $s = \sqrt{\sum_{i=1}^n\left(E_{EC}^i-E_{mod}^i\right)^2/\left(n-m\right)}$ and $\sigma = \sqrt{\sum_{i=1}^n\left(E_{EC}^i-\bar{E}_{EC}\right)^2/n}$– where, E_{EC} is the evaporation by the eddy covariance method, E_{mod} is evaporation by an indirect method; $\bar{E}$ is the mean evaporation, (mm d^{-1}); n is the length of the series, and m is the number of empirical coefficients in the relationships (equal to 2 in our case). The mean daily evaporation over the observational period and its error ($\sigma_{\bar{E}} = \frac{\sigma}{\sqrt{n}}$) were calculated following Rozhdestvenskiy and Chebotarev (1974).

4 Results

4.1 -Weather conditions and lake surface water temperature

During the 2017–2018, daily mean air temperatures ranged from –5.6 ºC and 2.4 ºC, while daily mean wind speeds varied between 1.3 m s^{-1} and 13.2 m s^{-1}. Throughout January and February 2018, the mean daily wind speed was 6.3 m s^{-1}, and the mean daily relative humidity was 54% (ranging from 39% to 77%). Relative humidity reached 90% and more on 3 January and 2 December 2018. In 2019–2020, daily mean air temperature ranged from –1.4 ºC to 2.6 ºC, with an average of 1.0 ºC. The daily mean of the air temperature fluctuations spanned –4.9 ºC and 5.1 ºC, and warmest days were observed in late December 2019. Mean mean humidity was 56% (varying between 43% and 77%), with daily maximums exceeding 90% on 25–26 December 2019. Mean daily wind speed ranged from 1.3 m s^{-1} to 9.5 m s^{-1}, averaging 5.9 m s^{-1} across the experiment period. The strongest wind events (speed reached 13.0 m s^{-1}) were observed on 8 December 2019 and 1 January 2020, and the weakest wind events (speed below 0.5 m s^{-1}) occurred on 21–25 December 2019 and 3 January 2020.

Throughout the experimental periods, both Lake Zub/Priyadarshini and Lake Glubokoe were warmer than the ambient air. Between 30 December 2017 and 9 February 2018, the mean daily LSWT at Lake Zub/ Priyadarshini was 3.9 ºC, which was 4.7 ºC higher than the mean air temperature (Fig. 4a). The temperature difference between the lake surface and the air varied from –0.5ºC (2–3 January 2018) to 10.0 ºC (25–26 January 2018). Similarly, from 7 December 2019 to 15 February 2020, the mean daily LSWT at Lake Glubokoe was 3.1 ºC (ranging from 0.6 ºC to 5.3 ºC); on average, the lake was 2.4 ºC warmer than the ambient air during this period (Fig. 4b). The largest temperature gradient between the LSWT and the air was observed on 25–26 December 2019.

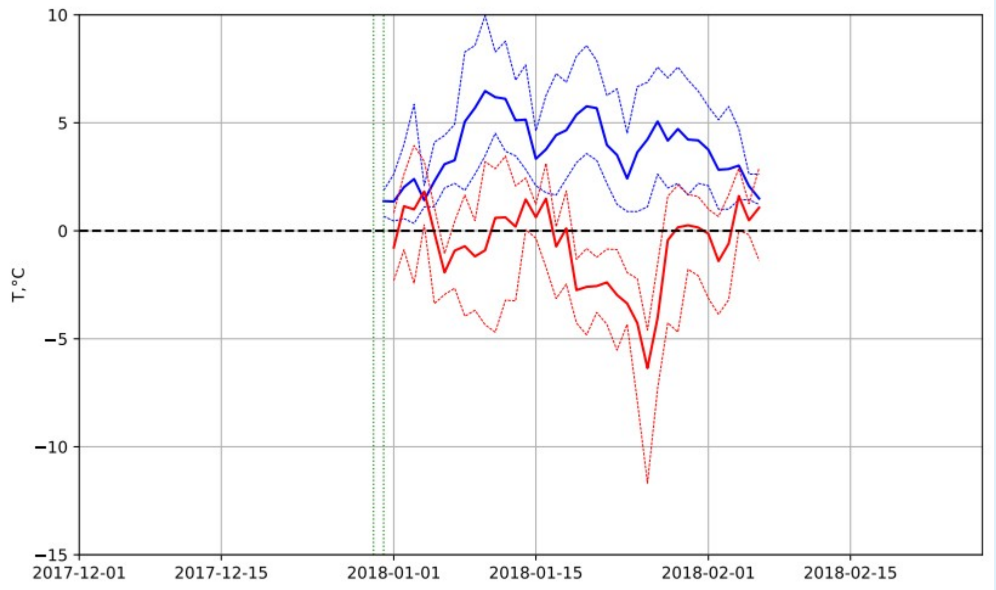

a

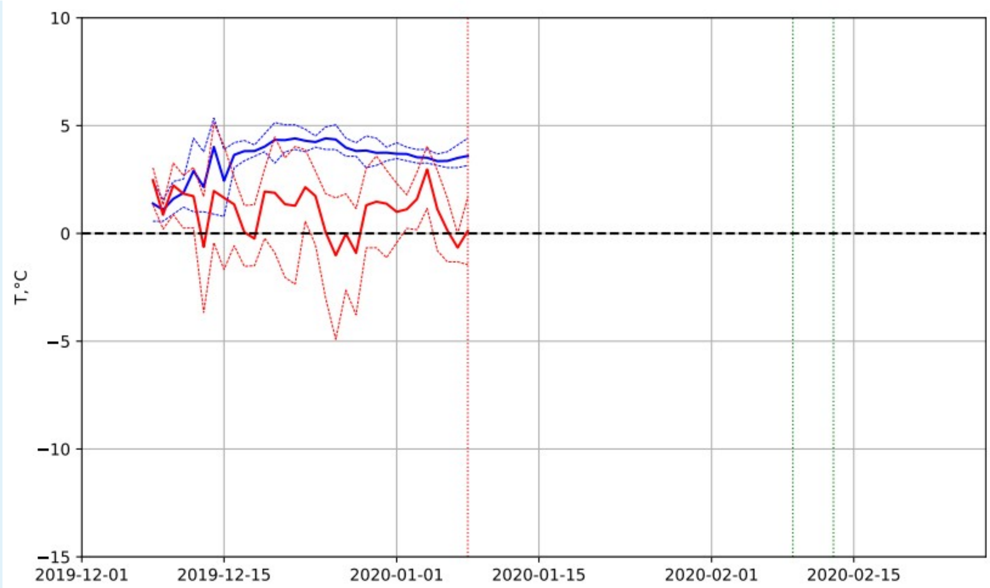

b

In 2017 – 2018, the weather was colder and less windy than the climatology (Table 1): the daily mean air temperatures ranged between –5.6 and 2.4 ºC , and the daily mean wind speed varied between 1.3 to 13.2 m s^{-1}. In January – February 2018, the mean daily wind speed was 6.3 m s^{-1}, and the daily mean relative humidity was 54 %, (varied between 39 and 77 %). The highest relative humidity (up to 90%) was observed on 3 January and 2 December 2018. In 2019 – 2020, the daily mean air temperature ranged from –1.4 ºC to 2.6 ºC, with an average of 1.0 ºC. The daily mean of the air temperature varied between –4.9 ºC to 5.1 ºC, and the warmest days were observed at the end of December 2019. The daily mean relative humidity was 56 %, and it varied between 43 % and 77 %; and the daily maximums exceeded 90 % on 25–26 December 2019. The daily mean wind speed ranged from 1.3 to 9.5 m s^{-1}, and averaged as 5.9 m s^{-1} for the period of the experiment (Table 2). The strongest winds (wind speed reached up to 13.0 m s^{-1}) were on 9 December 2019 and 1 January 2020, and the weakest winds (wind speed was less than 0.5 m s^{-1}) were on 21–25 December 2019 and 3 January 2020.

During most of the days in both experiments, Lake Zub/Priyadarshinis and Lake Glubokoe were warmer than the ambient air. During the period from 30 December 2018 to 9 February 2019, the mean daily LSWT in Lake Zub/Priyadarshini was 3.9 ºC, which was 4.7 ºC higher than the mean air temperature (Fig. 4 a). The difference between the LSWT and air temperature varied from –0.5 ºC (2–3 January, 2018) to 10 ºC (25–26 January, 2018). From 7 December 2019 to 15 February 2020, the mean daily LSWT of Lake Glubokoe was 3.1 ºC, ranging from 0.6 to 5.3 ºC. During this period, the lake was 2.4 ºC warmer than the air on average (Fig. 4 b). The largest difference between the LWST and air temperature was observed on 25–26 December 2019, when also the relative humidity was the highest, exceeding 90 %.

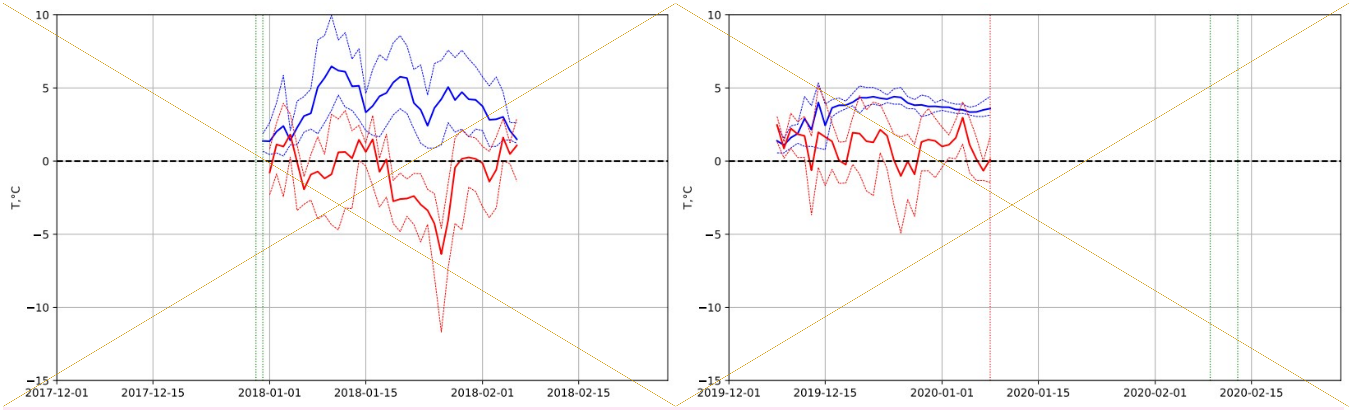

~~a~~ ~~b~~

Figure 4: Daily ~~. The daily~~ minimum, mean and maximum for the air temperature (red lines) and LSWT (blue lines) measured during the experiments on Lake Zub/Priyadarshini (a) and Lake Glubokoe (b). In (b) the red line shows 8 ~~day 8 in~~ January 2020. The green lines in (a and b)~~boxes~~ show the days when the lakes became free of ice.

4.2 Eddy-covariance

Direct measurements of evaporation were a key component of this study. The open-path EC system was installed on a location allowing it to cover the lake surface sector which was between 105 and 240 degrees for Lake Zub/Priyadarshini, and between 90 and 225 degrees for Lake Glubokoe (green lines on Fig. 5). Fig. 5 a and b show ~~the~~ radial histograms (bar charts~~a bar chart~~ given around a circle) for the two experiments, where the height of the bars~~bar~~ represents the frequency (number of cases) and the colour segments within each bar represent the mean wind speed. During the Lake Zub/Priyadarshini experiment, ~~mean wind speeds ranged from 3.5 to 7.5 m s^{-1},~~ and in the most frequent sector the mean wind speed was of~~it was approximately~~ 6.5 m s^{-1}. At Lake Glubokoe, a maximum wind speed of ~~mean speeds ranged from 3.5 to~~ 5.5 m s^{-1} ~~, with a maximum wind speed~~ observed in the most frequent sector of wind directions. In Fig. 5 c and d, the radial histograms show the XR_{90} (m) representing the horizontal distance over the lake surface that encompasses 90 % of the flux footprint. During the Lake Zub/Priyadarshini experiment, mean XR_{90} ranged from 95 to 135 m, and in the most frequent sector it was approximately 120 m. For the Lake Glubokoe, the mean XR_{90} ranged from 70 to 190 m, with a value of approximately 90 m in the most frequent sector.

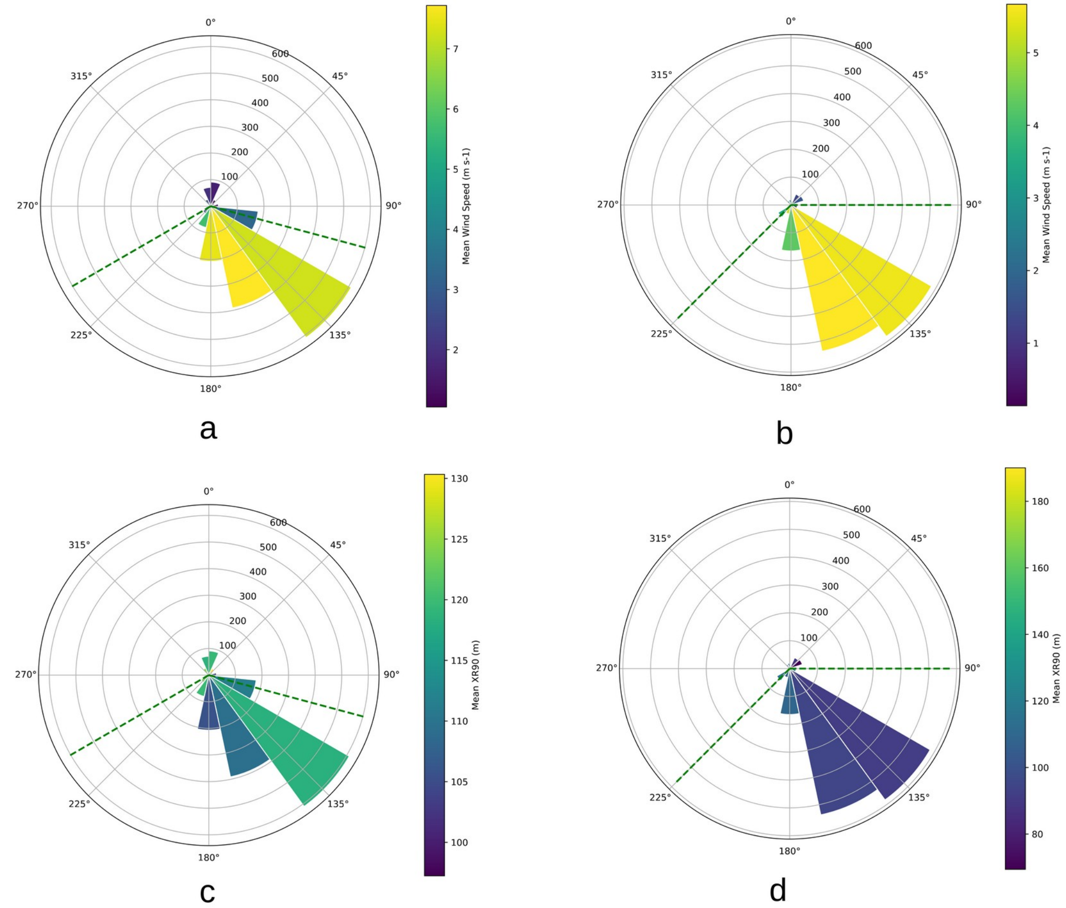

Figure 5:~~.~~ The wind speed and direction measured at IRGASON~~Irason~~ site (a: Lake Zub/Priyadarshini, and b: Lake Glubokoe) and the footprint length estimate (XR_{90}~~X90~~, m) (c: Lake Zub/Priyadarshini, and d: Lake Glubokoe). The green lines indicate the footprint sector.

The installation height of the IRGASON system (1.8–2 m) creates a "blind zone" surrounding the instrument, ensuring that the shoreline and its surrounding terrain do not interfere with the flux measurements. Furthermore, this low installation height ensures that the vertical divergence of the water vapour flux remains negligible. The raw 30-minute measurements were filtered based on the sensor signal strengths, data gaps, footprint modelling and the specific wind direction sectors covering the lake. Less than 20% of the total data were excluded; the majority of these exclusions resulted from wind directions originating outside the lake sector. These gaps were replaced by mean evaporation estimated for the experimental period. Hourly, daily and seasonal cumulative sum were further calculated from the filled data. Figure 6 illustrate the filtered evaporation that were excluded from analysing in the experiment on Lake Glubokoe (2019–2020) where red lines delineate sector of wind directions covering the lake surface (a) and the red dots represent the filtered data points (b).

The IRGASON height of 1.8 – 2 m generates a blind zone near the instrument, so that the stones on the downwind shore do not affect the fluxes. The low height of the instrument also guarantees that the vertical divergence of the water vapour flux is negligible. The raw 30-minute measurements were filtered by the sensors' signal strengths, a number of gaps in the observations, the footprint and the sector of wind directions covering a lake. The percentage of the filtered out (excluded) measurements did not exceed 20 % of total data, and most of the excluded data corresponded to wind directions outside a lake. The gaps were replaced by the mean of evaporation estimated for the period of the experiment, and the hourly and daily cumulative sum were calculated from the data with gaps filled. Figure 6 shows how the values of evaporation were filtered in the experiment on Lake Glubokoe (2019 – 2020): the red lines outline the sector of wind directions covering the lake surface (a), and the red dots show the filtered values (b).

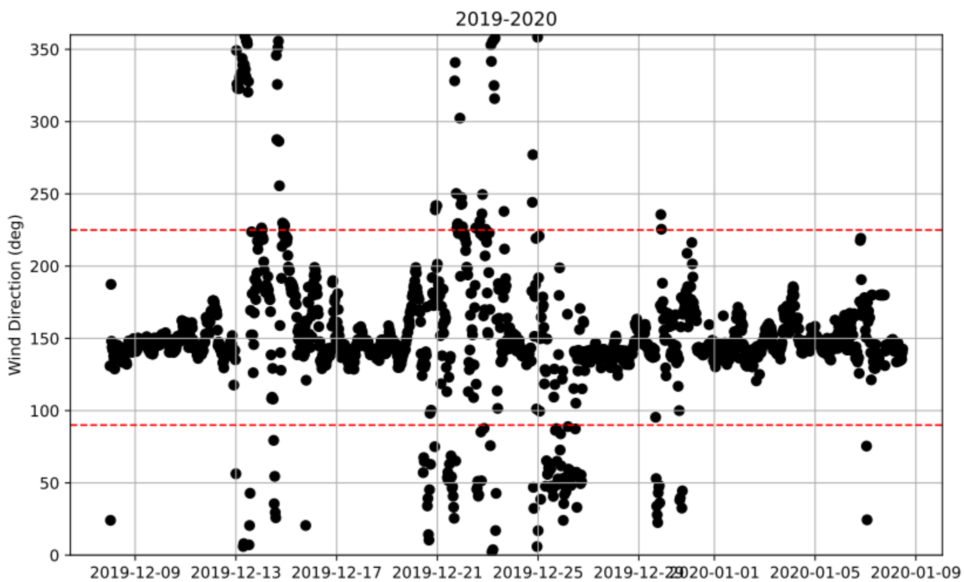

a

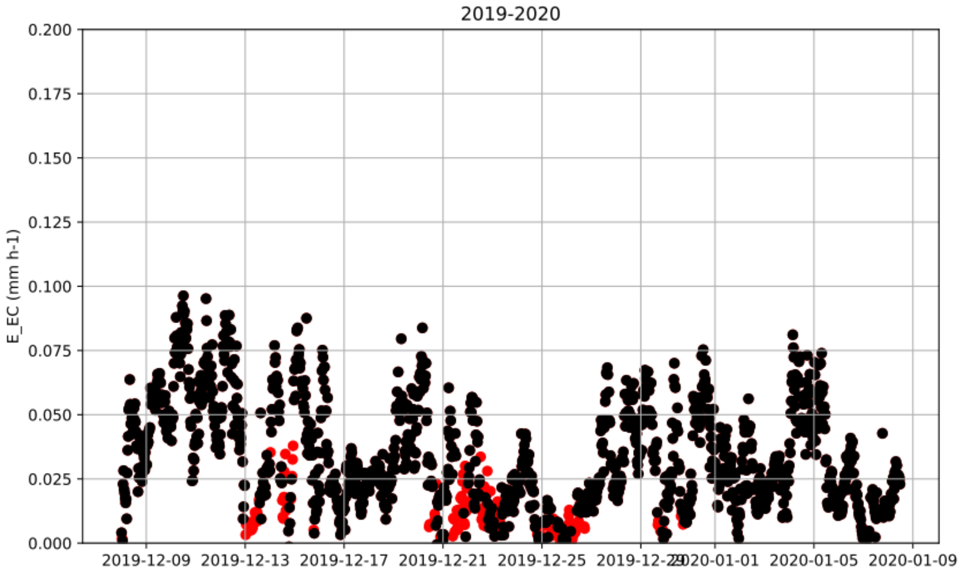

b

Figure 6:~~Fig. 6.~~ The 30-minute means of the wind direction (a) and evaporation (b) measured by the EC instrumentation on Lake Glubokoe. On (a): the red lines show the limit of the wind directions within the footprint; on (b): the red dots indicate the measurements collected outside the foot.

For Lake Zub/Priyadarshini, daily mean evaporation rate varied from 1.5 mm d^{-1} to 5.0 mm d^{-1} with an average of 3.0 ± 0.3 mm d^{-1}. This average was derived by dividing the total evaporated water (114 mm) by the duration of the experiment (38 days). Evaporation rates increased with wind speed, peaking at 5.0 mm d^{-1} during the storm event on 2–3 January 2018. For Lake Glubokoe, the daily mean evaporation rate varied between 0.3 and 3.2 mm d^{-1}, averaging 1.5 ± 0.1 mm d^{-1} with a cumulative total of 54 mm over the experimental period. The highest evaporation rates (> 2.5 mm d^{-1}) occurred on 9–11 December 2019 and 3–4 January 2020, while the lowest rates (< 0.9 mm d^{-1}) were observed on 6–7 January 2020.

~~The daily mean evaporation rate as well as the cumulative sum for the whole period were calculated from high-frequency measurements. For Lake Zub/Priyadarshini, the daily mean evaporation rate varied from 1.5 to 5.0 mm day^{-1} and took an average 3.0 ± 0.3 mm day^{-1}. The average daily evaporation rate was calculated by dividing 114 mm of evaporated water (sum over the whole period of the experiment) by the number of days in the period (which is 38). The evaporation increased with wind speed, with the maximum of 5.0 mm d^{-1} observed during the storm on 2–3 January 2018. For Lake Glubokoe, the daily mean evaporation rate varied between 0.3 and 3.2 mm d^{-1}, and took on average 1.5 ± 0.1 mm d^{-1}. The total sum of the evaporation in this experiment was 54 mm. The largest evaporation (> 2.5 mm d^{-1}) was observed on 9–11 December 2019 and 3–4 January 2020. The smallest evaporation (< 0.9 mm d^{-1}) was observed on 6–7 January 2020.~~

4.3 Empirical formulas

Evaporation was estimated using four empirical formulas: the resulting mean daily evaporation rates ranged from 0.4 ± 0.1 mm d^{-1} to 1.1 ± 0.1 mm d^{-1}, representing values 27–73% lower than those derived from the eddy covariance method (Table 3). The formula proposed by Shevnina et al. (2022) yielded a daily mean evaporation rate of 1.5 ± 0.2 mm d^{-1} for the ice-covered Lake Glubokoe (based on independent data), which is only 6% lower than the rate calculated via the EC technique. Overall, the performance of these formulas was suboptimal: the ratio of the standard deviation of the error (s) to the standard deviation of the observations (σ) was $s/\sigma > 2$, and the root-mean-square error (RMSE) reached 2.2 mm d^{-1}.

~~The evaporation over the was estimated on the basis of four formulas: the mean daily evaporation varied between 0.4 ± 0.1 mm d^{-1} and 1.1± 0.1 mm d^{-1}, which represent 27 – 73 % less than the evaporation based on the EC method (Table 3). The formula by Shevnina et al. (2022) gave the daily mean evaporation of over 1.5 ± 0.2 mm d^{-1} over the ice-covered Lake Glubokoe (independent data); it is only 6% less with respect to the evaporation rate calculated from the EC technique. The scores of all formulas are weak: $s/\sigma > 2$, and the RMSE is up to 1.6 mm d^{-1} (Table 4).~~

Table 3. The evaporation over two glacial lakes on the basis of the empirical~~emirical~~ formulas and their skill scores. The daily mean evaporation in mm d^{-1} , and the cumulative sum is given in mm $period^{-1}$.

Author(s) in Table 3	Lake Zub/ Priyadarshini			Lake Glubokoe		
	Mean	Sum	RMSE / s/σ	Mean	Sum	RMSE / s/σ
Penman (1948)	1.3 ± 0.2	48	1.8 / 2.0	0.6 ± 0.1	20	1.3 / 2.1
Doorenbos and Pruitt (1975)	1.8 ± 0.2	68	1.3 / 1.6	0.8 ± 0.1	28	1.5 / 2.4
Odrova (1979)	0.8 ± 0.1	32	2.2 / 2.4	0.4 ± 0.1	13	1.3 / 2.2
Shuttleworth (1993)	1.0 ± 0.1	38	2.1/ 2.3	1.1 ± 0.1	37	1.3 / 2.1

4.4 Bulk-aerodynamic method

We estimated the lake evaporation on the basis of the observed wind speed, lake surface temperature ~~(controlling q_S)~~, and air specific humidity, applying three literature based formulae for C_{EzN}~~C_{ENz}~~ (Heikinheimo et al., 1999; Arya, 1988; Andreas, 1986). In addition, the actual values of the transfer coefficient were derived from the direct observations on evaporation, wind speed, air specific humidity, and surface saturation specific humidity collected during the experiment on Lake Zub/Priyadarshini (2017–~~—~~2018). Using~~Applying~~ Eq. (1), 30-minute mean values of C_{E2} were solved on the basis of the observed evaporation~~E~~, q_S, q_2 and w_2~~, and the results were converted to CEN2~~. Finally, to facilitate comparison with literature-based relationships ~~allow comparison against relationships presented in the literature~~ for the standard height of 10 m, we converted the C_{E2N} values to C_{E10N} ~~the CEN2 values were converted to CEN10 values~~ applying the iterative algorithm of Launiainen and Vihma (1990). The result ~~-~~demonstrated an approximately piecewise~~piecevise~~ linear relationship between w_2 and C_{EzN} (Fig. 7~~C_{EN} (Figure 10~~). Linear regressions were derived for the wind regimes below and above 13 m s^{-1}), separately for C_{E10N} and C_{E2N}~~CEN10 and CEN2~~ as follows:

C_{E10N}~~C_{EN10}~~ $= 0.0000119\, w_2 + 0.00114$ (if $w_2 < 13$ m s^{-1}), (15)

$C_{E10} = 0.0013$ (if $w_2 >= 13$ m s^{-1}). (16)

C_{E2N}~~C_{EN2}~~ $= 0.0000193\, w_2 + 0.00153$ (if $w_2 < 13$ m s^{-1}), (17)

$C_{E2} = 0.0018$ (if $w_2 >= 13$ m s^{-1}), (18)

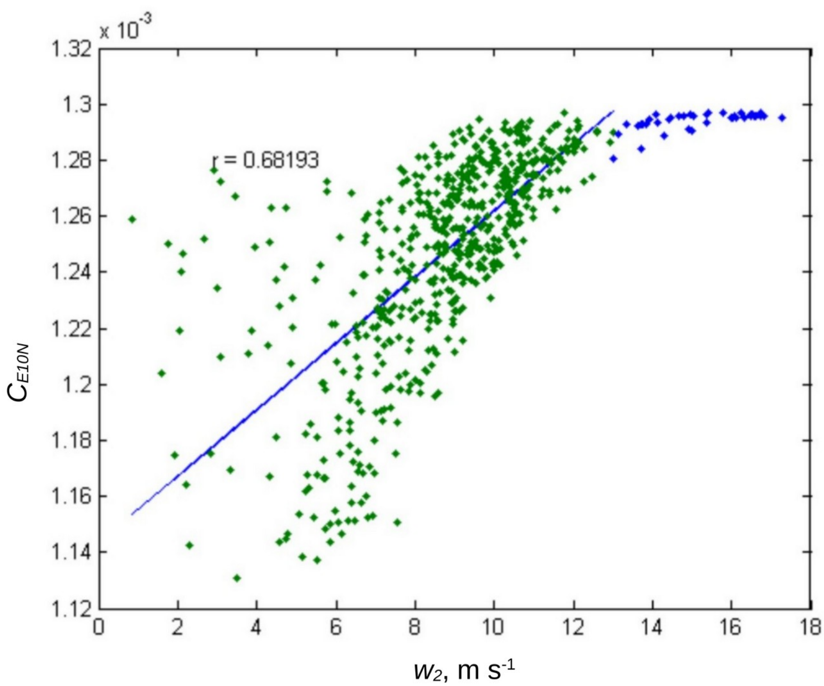

Figure 7:~~Fig. 7.~~ Dependence of the 10-m neutral transfer coefficient for moisture (C_{E10N}~~C_{EN10}~~) on the 2-m wind speed (w_2~~w2~~) on the basis of 30-minute mean values observed over Lake Zub/Priyadarshini (2017–2018).

Lake ~~The lake~~ evaporation measured via~~with~~ the EC technique inherently includes ~~includes the~~ contributions of both interfacial evaporation at the water~~from the lake~~ surface and evaporation from spray air droplets. Although distinguishing ~~droplets in the air. It is difficult to distinguish~~ between these two components is challenging,~~contributions but, based on~~ observations by Guest (2021) over the Southern Ocean suggest ~~, we may assume~~ that under high-wind conditions, ~~very strong winds the~~ spray evaporation may account for approximately 18~~is some 18~~ % of ~~the~~ interfacial evaporation. Consequently~~Accordingly~~, if one wants to apply the wind dependent transfer coefficient (Eqs. 17 and 18) solely for the interfacial evaporation, the contribution of spray evaporation must be subtracted from the results. Furthermore, the ~~The~~ stability dependence of the moisture ~~for the~~ transfer coefficient was found to be ~~of moisture was~~ minor. This is primarily because the lakes consistently remained~~was because during the period of the experiments, the lakes were continuously~~ warmer than the ambient air during the period of the experiments (e.g., an average difference of ~~(on average by~~ 4.7 °C in January–~~ – ~~February 2018). Consequently, under high-wind conditions, atmospheric stability remained near-neutral, rendering~~Hence, when the wind was strong, the stratification was close to neutral and~~ the transfer coefficient ~~was~~ large and relatively insensitive to stability variations. ~~not sensitive to the stratification.~~

The actual values of the transfer coefficients (C_E and C_D) were estimated from EC measurements at Lake Glubokoe (2019–2020) using the methods described by Arya (1988) and Andreas (1986). In the first method (Eqs. 3–12), coefficients were estimated using roughness lengths derived from literature-based friction velocities (shown as black dots in Fig. 8). In the second method (Eqs. 13–14), transfer coefficients were calculated independently of atmospheric stability and friction velocity (shown as red dots in Fig. 8).

~~The actual values of the transfer coefficients (C_E and C_D) were estimated from the EC measurement on Lake Glubokoe (2019 – 2020) applying the methods referred to Arya 1988 and Andreas 1986 (Table 2). In the first method (Eqs. 3 - 12), the actual values were estimated for the roughness lengths calculated with literature-based friction velocity (black dots in Fig. 8). In the second method (Eqs. 13–14), the actual values of the transfer coefficients were calculated with independence of stability and friction velocity (red dots in Fig. 8) .~~

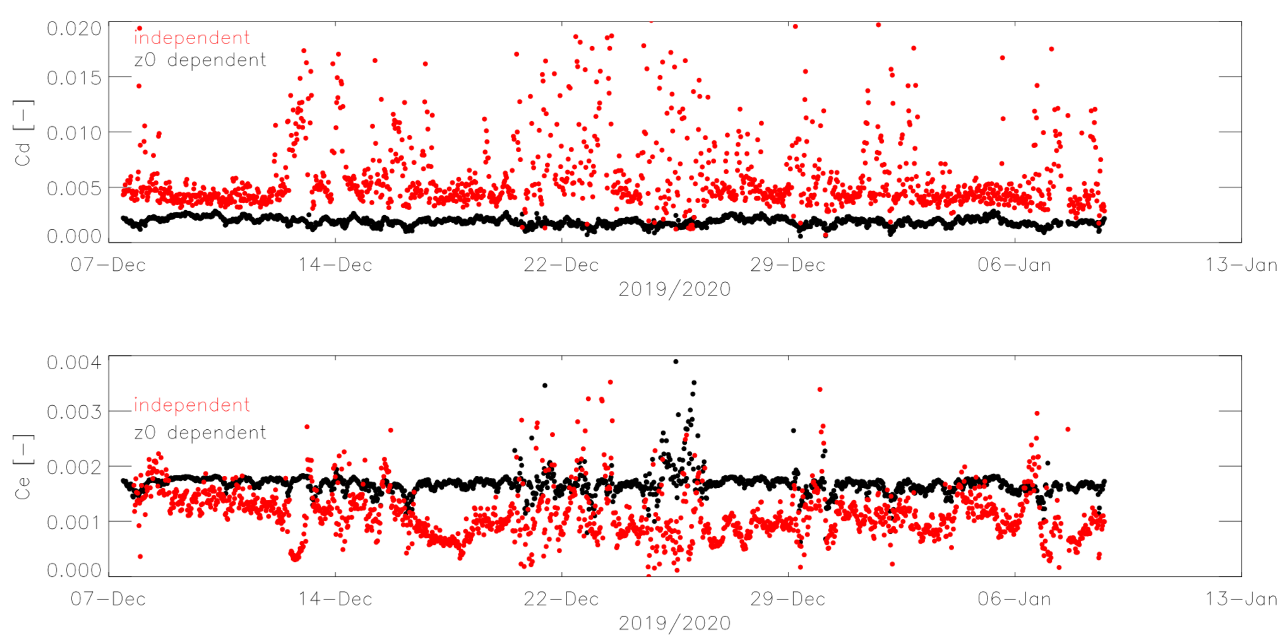

Figure 8:Fig. 8. The actual values of the bulk transfer coefficients calculated following Arya 1988 (black dots) and Andreas 1986 (black dots) estimated from the EC measurement on Lake Glubokoe (2019–2020).

The actual values for C_{E10} (normalized to a standard height of 10 m) varied between $1.2\cdot10^{-3}$ and $2.1\cdot10^{-3}$. Table 4 presents these values adjusted to our specific instrumentation heights: 2 m for Lake Zub/Priyadarshini and 1.8 m for Lake Glubokoe. These C_{Ez} values were subsequently used to calculate lake evaporation via Eq. (1). We evaluated the performance of the bulk-aerodynamic method with simulating hourly, daily, and seasonal cumulative evaporation totals based on the 30 minute EC data.

The actual values for the C_{E10} (for the standard height of 10 meters) varied between $1.1\cdot10^{3}$ and $2.1\cdot10^{3}$, in Table 4 they are given for the height of our instrumentation: 2 m for Lake Zub / Priyadarshini and 1.8 m for Lake Glubokoe. The values of the C_{Ez} were further used in calculations of lake evaporation with the Eq. (1), and estimations of the scopes for the bulk-aerodynamic method simulating the hourly, daily and seasonally cumulative sums of lake evaporation calculated from the 30 minute data.

Table 4. The equations applied in estimations the transfer coefficient (C_E) in the bulk-aerodynamic method. Notations: *N* refers to the neutral stratification, and *z* refers to the height of the instrument.

Lake	Eqs. for the C_E	Methods	C_{EzN}	
			z = 10 m	*z* = [1.8–2] m
Lake Zub / Priyadarshini (2017–2018) Lake Glubokoe (2019–2020)	from literature	Heikinheimo et al., 1999	$1.2\cdot10^{-3}$	$1.1\cdot10^{-3}$
Lake Glubokoe (2019–2020)	Eqs. (17–18)	Wind dependent	$1.5\cdot10^{-3}$	$1.3\cdot10^{-3}$
Lake Zub / Priyadarshini (2017–2018)	Eqs. (3–12)	Arya, 1988	$1.4\cdot10^{-3}$	$1.2\cdot10^{-3}$
	Eqs. (13–14)	Andreas, 1986	$2.1\cdot10^{-3}$	$1.7\cdot10^{-3}$

Lake	Eqs. for the C_E	Methods	$C_{E\,Nz}$	
			z = 10 m	*z* = [1.8 – 2] m
Lake Zub / Priyadarshini (2017 – 2018) Lake Glubokoe (2019-2020)	taken from literature	Heikinheimo et al., 1999	1.2×10^{-3}	1.1×10^{-3}

~~Lake Glubokoe (2019–2020)~~	~~Eqs. (17 – 18)~~	~~Wind dependent~~	~~1.5×10^{-3}~~	~~1.3×10^{-3}~~
~~Lake Zub / Priyadarshini (2017 – 2018)~~	~~Eqs. (3 – 12)~~	~~Arya, 1988~~	~~1.4×10^{-3}~~	~~1.2×10^{-3}~~
	~~Eqs. (13 – 14)~~	~~Andreas, 1986~~	~~2.1×10^{-3}~~	~~1.7×10^{-3}~~

The hourly ~~rate of~~ lake evaporation rate was simulated using~~with~~ the bulk-aerodynamic method, applying the transfer coefficients C_{Ez} determined in Table 4 ~~following the different actual values of the E_{C2} (Table 4)~~. Figure 9 demonstrates strong ~~shows a good~~ agreement between the bulk-aerodynamic simulations and the independent eddy covariance (EC) ~~independent~~ measurements: the Pearson correlation coefficient is 0.92 for the data collected at ~~in the experiments on~~ Lake Zub/Priyadarshini during the 2017–2018 experiment ~~, 2017 – 2018~~ (Fig. 9a~~9 a~~) and 0.89 for Lake Glubokoe during the 2019–2020 experiment ~~Gluboke, 2019 – 2020~~ (Fig. 9b).~~9 b).~~

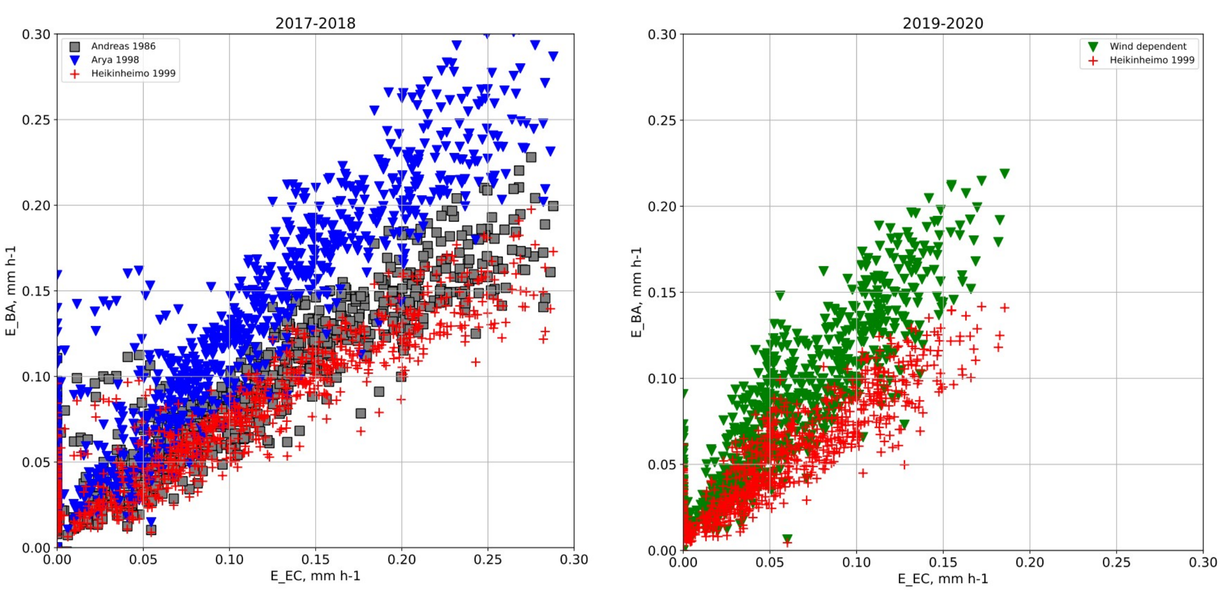

a b

Figure:~~Fig.~~ 9. The measured (x-axis) evaporation and simulated (y-axis) with the bulk-aerodynamic method applying different actual values for the C_E~~$_{EC}$~~: (a) Lake Zub/Priyadarshini and (b) Lake Glubokoe. The red dots cross to Heikinheimo et al. (1999), grey box to Andreas (1986), blue triangle to Arya (1988), and green triangle to the wind-dependent coefficient.

Lake evaporation is primarily driven by two factors: the vapour pressure deficit (which depends on the surface-air temperature gradient) and wind speed. Results from the two studied lakes indicate no significant dependency between lake evaporation and the vapour pressure deficit (Fig. 10a), with Pearson correlation coefficients near zero for both experimental periods (2017–2018 and 2019–2020). Conversely, a strong dependence was observed between lake evaporation and wind speed (Fig. 10b), with Pearson correlation coefficients of 0.58 for the ice-free Lake Zub/Priyadarshini (2017–2018) and 0.75 for the ice-covered Lake Glubokoe (2019–2020). These results imply that wind speed is the primary driver of evaporation for these lakes.

~~There are two factors driving lake evaporation: the vapor pressure deficit (depends on a land surface-air temperature gradient) and wind speed. The results from two glacial lakes suggest no dependency between the lake evaporation and the vapor pressure deficit (Fig. 10 a) with the Pearson correlation coefficient is near zero in both experiments (2017 – 2018 and 2019 – 2020). However, the dependence between the lake evaporation and the wind speed is strong (Fig. 10 b), the Pearson correlation coefficient is 0.58 for the ice-free Lake Zub/Priyadarshini (2017 – 2018) and is 0.75 for the ice-covered Lake Glubokoe (2019 – 2020). It implies that the wind speed is the major driver for the evaporation over the local lakes.~~

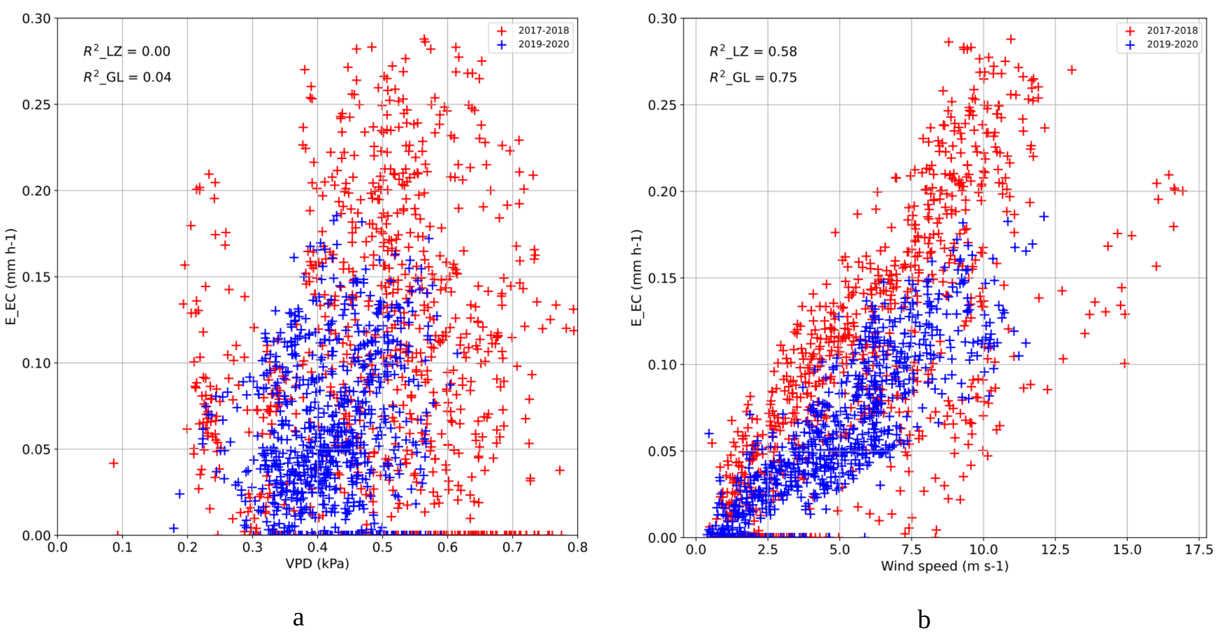

Figure 10: The scatter plots ~~scatterplots~~ of the vapour~~vapor~~ pressure gradient, (x-axis in a: VPD, kPa) and wind speed (x-axis in b: m s^{-1}) against the hourly rate of lake evaporation (y-axis in a and b) for Lake Zub/Priyadarshini (red) and Lake Glubokoe (blue).”

The daily and seasonal rate of lake evaporation were calculated as the~~a~~ cumulative sum of ~~the~~ hourly rate after the bulk-aerodynamic method using various C_{E2} values~~(with the various C_{E2})~~. For the ice free Lake Zub/Priyadarshini (2017–2018), the mean daily evaporation rate varied between 2.0 ± 0.1 mm d^{-1} and 3.0 ± 0.2 mm d^{-1} (Table 5). The best agreement with the EC technique (3.0 ± 0.2 mm d^{-1}) was achieved using ~~scores for the daily mean evaporation rate gives the~~ C_{E2} = 1.7·10^{-3}. For Lake Glubokoe (2019–2020), the optimal estimate for the mean daily evaporation rate of 1.5 ± 0.1 mm d^{-1} is obtained using a transfer coefficient of C_{E2} = 1.2·10^{-3}. This yields a daily lake evaporation rate of 1.6 ± 0.1 mm d^{-1}, which is approximately 8% lower than the reference (EC) method. Depending on the chosen value of C_E, the bulk-aerodynamic method either underestimated evaporation by up to 20% (at C_{E2} = 1.1 x 10^{-3}) or overestimated it by up to 38% (using Eq. 17). The root-mean-square error varied between 0.4 mm d^{-1} and 0.8~~x 10^{-3}, and it fits the estimates according to the EC technique (3.0 ± 0.2~~ mm d^{-1}, and the s/σ ratio was 0.7 for C_{E2} values of 1.2·10^{-3} and 1.7·10^{-3}. These scores are considered acceptable for an indirect method, satisfying the criterion of s/σ < 0.8.~~).~~

Table 5. The lake evaporation estimated using the bulk-aerodynamic method used different ~~actual~~ values of the transfer coefficient (C_{E2}). The bold numbers indicate the indirect method that yielded the estimates closest to the reference, and the parentheses show the verification with the independent data. ~~Sum is the cumulative value for the period of the experiment (Table 2).~~

The C_{E2} values	Lake Zub/ Priyadarshini (2017–2018)			Lake Glubokoe (2019–2020)		
	Mean mm d^{-1}	Sum mm	RMSE / s/σ	Mean mm d^{-1}	Sum mm	RMSE / s/σ
1.1· 10^{-3}	[2.0 ± 0.2]	[78]	[1.0 / 1.1]	[1.3 ± 0.1]	[42]	[0.5 / 0.8]
1.3· 10^{-3}	2.6 ± 0.2	100	0.7 / 0.7	[1.9 ± 0.2]	[63]	[0.5 / 0.9]
1.2· 10^{-3}	[2.1 ± 0.2]	[79]	[0.9 / 0.9]	**1.5 ± 0.1**	**50**	**0.4 / 0.7**
1.7· 10^{-3}	**[3.0 ± 0.2]**	**[114]**	**[0.7 / 0.7]**	2.2 ± 0.2	71	0.8 / 1.2

~~Actual value the C_{E2} in Table 5~~	~~Lake Zub/ Priyadarshini (2017 – 2018)~~			~~Lake Glubokoe (2019 – 2020)~~		
	~~Mean mm d^{-1}~~	~~Sum mm~~	~~RMSE / s/σ~~	~~Mean mm d^{-1}~~	~~Sum mm~~	~~RMSE / s/σ~~
~~1.1 x 10^{-3}~~	~~[2.0 ± 0.2]~~	~~[78]~~	~~[1.0 / 1.1]~~	~~[1.3 ± 0.1]~~	~~[42]~~	~~[0.5 / 0.8]~~
~~Eqs. (17, 18)~~	~~2.6 ± 0.2~~	~~100~~	~~0.7 / 0.7~~	~~[1.9 ± 0.2]~~	~~[63]~~	~~[0.5 / 0.9]~~

~~1.2 x 10^{-3}~~	~~[2.1 ± 0.2]~~	~~[79]~~	~~[0.9 / 0.9]~~	~~**1.5 ± 0.1**~~	~~**50**~~	~~**0.4 / 0.7**~~
~~1.7 x 10^{-3}~~	~~**[3.0 ± 0.2]**~~	~~**[114]**~~	~~**[0.7 / 0.7]**~~	~~2.2 ± 0.2~~	~~71~~	~~0.8 / 1.2~~

~~For Lake Glubokoe (2019 – 2020), the best estimate for the evaporation being 1.5 ±0.1 mm d^{-1} (on average) is obtained with the transfer coefficient C_{E2} = 1.2 x 10^{-3} with the daily lake evaporation of 1.6 ± 0.1 mm d^{-1}; it is approximately 8% less than the reference method. Depending on the value of transfer coefficient (C_E), the bulk-aerodynamic method either underestimated the evaporation up to 20% (1.1 x 10^{-3}) or overestimated it up to 38% (Eqs. 17). The RMSE varied from 0. 4 to 0.8 mm d^{-1}, and the s/σ criteria was 0.7 when the C_E was 1.2 x 10^{-3} and 1.7 x 10^{-3}, and the scores are acceptable for an indirect method (s/σ < 0.8).~~

It is indeed interesting that the new wind-dependent transfer coefficient, derived on the basis of Lake Zub/Priyadarshini data, has a smaller RMSE for Lake Glubokoe than for Lake Zub/Priyadarshini. This is, however, understandable because the transfer coefficient is only one of the factors that controls the evaporation calculated using the bulk-aerodynamic formula. ~~(Eq. (1)).~~ In addition to the transfer coefficient, at least the following factors may generate inaccuracy in the estimated evaporation: (1) errors in the measurements of lake surface temperature (controlling the saturation specific humidity), air specific humidity, and wind speed, (2) contribution of spray droplets to evaporation, (3) role of waves in the lake surface, and (4) validity of the Monin-Obukhov similarity theory, which requires quasi-stationary, horizontally homogeneous conditions. Errors and uncertainties associated with (1)–(4) above may either increase the overall error or partially offset one another. Hence, it is reasonable that the actual value of the transfer coefficient varies among lakes, as factors (1)–(4) may be site-specific, and also depends on the metrics used to evaluate performance (e.g., RMSE or *s/σ*~~) to evaluate performance (Table 3~~).

5 Discussion

The eddy covariance technique is widely recognized as the most precise method for directly measuring evaporation over inland waters (Eugster et al., 1997; Spank et al., 2020; Rodrigues et al., 2020) and is commonly used as a reference to validate indirect methods (Tanny et al., 2008; Wang et al., 2019). However, its accuracy is sensitive to how the measurement system is deployed and post-processed (Burba, 2013; Spank et al., 2025). In our experiments, the EC system was deployed at low heights (1.8–2 m) to measure fluxes over the lake surface. The system was positioned to account for prevailing winds, and throughout the experiments, more than 80% of the measured fluxes originated from the lake surface footprint. The EC measurements were processed using standard routines for open-path systems (filtering, gap filling, and footprint analysis). Therefore, we considered the EC measurements as the reference against which we compared the lake evaporation calculated via the indirect methods.

We estimated lake evaporation using eddy covariance measurements collected at two field experiments which spanned the ice break-up and ice-free periods for two glacial lakes differing in depths, volumes, and thermal regimes. For Lake Zub/Priyadarshini, direct estimates yielded a mean daily evaporation rate of 3.0 ± 0.2 mm d^{-1} during the ice-free period (January–February 2018). Daily evaporation rates ranged from 1.5 mm d^{-1} to 5.0 mm d^{-1}, with a cumulative total of 114 mm over the 38-day study period (1 January to 7 February 2018). Evaporation rates showed a strong positive correlation with wind speed, peaking at 5.0 mm d^{-1} during storm events, with the highest values recorded on 2–3 January 2018. For Lake Glubokoe, daily evaporation rates varied between 0.3 mm d^{-1} and 3.2 mm d^{-1}, averaging 1.6 ± 0.1 mm d^{-1} during the ice break-up period. The cumulative evaporation for this 33-day period (December 2019–January 2020) was 54 mm, with the largest rates (up to 3.0 mm d^{-1}) observed during a storm on 13–15 December 2019. The EC measurements suggest that lakes begin significant evaporation immediately following break-up. The evaporation process is likely driven by strong and cold winds that maintain high evaporation rates even when the vapour pressure gradient is low.

~~The EC technique has been recognized as the most precise for directly measuring the evaporation over inland water (Eugster et al., 1997; Spank et al., 2020; Rodrigues et al., 2020), and has taken as a reference to quantify various indirect methods (Wang et al., 2019; Tanny et al., 2008). Its accuracy is, however, sensitive to how a measuring system has been deployed and post-processed (Spank et al, 2025; Burba, 2013). In our experiments, the EC system was deployed to measure fluxes over the lakes on low heights (1.8 – 2m), and the data got low gaps. The system was deployed with accounting the prevailing winds, and during the experiments the instrumentation fetched up to more than 80 % fluxes from the footprint covered by a lake surface. The EC measurements were processed following the standard routine for the open-path systems (filtering, gap filling and footprint). Therefore, we considered the EC measurements given the reference to compare the lake evaporation calculated with the indirect methods.~~

~~We estimated evaporation from the EC measurements collected in two lakes in the Schirmacher Oasis. Two field experiments covered the break-up and ice-free periods on the lakes differing in depth, volume and thermal regime. For Lake Zub/Priyadarshini, the direct estimates give the average daily evaporation rate as 3.0 ± 0.2 mm d^{-1} in January – February 2018 when the lake was ice-free. The daily evaporation varied from 1.5 to 5.0 mm day^{-1}; and the cumulative sum of lake evaporation was 114 mm for the period from 1 January to 7 February 2018 (38 days). The evaporation increased with the wind speed, and took the maximum of 5.0 mm d^{-1} observed during storms. The highest evaporation was measured on 2 – 3 January 2018. For Lake Glubokoe, the daily evaporation rate varied between 0.3 and 3.2 mm d^{-1}, with an average of 1.6 ± 0.1 mm d^{-1} during the ice break-up period. The cumulative sum of evaporation is 54 mm of evaporation over the 33-day period in December 2019 – January 2020. The largest evaporation rate (up to 3.0 mm d^{-1}) was observed during the storm 13–15 December 2019. The EC measurements imply the lakes start evaporating immediately after the break up, and this effect is likely caused by the strong winds resulting in the high evaporation rate even in days with low vapour pressure gradient.~~

To the best of our knowledge, ~~the~~ measurements of lake evaporation in Antarctica using~~with~~ the EC technique have been conducted only at~~were done only on~~ two lakes in the Schirmacher Oasis. However, such~~these~~ measurements are available for natural and artificial lakes globally (Guseva et al., 2022; Liu, 2023). While many studies analyse the surface energy budget of lakes, they typically report evaporation as a latent heat flux expressed in W m^{-2} or J cm^{-2} day^{-1} (Stewart and Rouse, 1976; Stannard and Rosenberry, 1991; Blanken et al.~~Marsh and Verseghy~~, 2000; Oswald and Rouse, 2004; Blanken et al., 2011). These energy-based units are ~~often~~ impractical for hydrological (water balance) applications~~,~~ and are difficult to compare directly with evaporation depths measured by other techniques (e.g.~~for example~~, evaporation pans). To ensure the comparability of our results, we converted the reported latent heat fluxes (W m^{-2}) into equivalent depths of evaporated water.

Eddy covariance measurements remain rare for lakes located north of 60° latitude. Ala-Könni et al. (2022) measured evaporation over Lake Kuivajärvi (61°N, Finland) during the ice-free period, reporting a mean evaporation rate of 1.5–2.5 mm d^{-1} during July–August; peak values of up to 5.0 mm d^{-1} were observed during days with strong winds or when dry, cold synoptic fronts passed over the site. Blanken et al. (2000, 2003) measured evaporation over Great Slave Lake (62°N, Canada) during the ice-free periods from June to September (1997–1999), where evaporation rates reached 2.8 mm d^{-1}. Granger and Hedstrom (2011) estimated that the 4–9-day averaged evaporation rate reached 3.2–3.9 mm d^{-1} during the ice-free period for small lakes situated next to Great Slave Lake. The northernmost EC measurements were collected from a small Arctic thermokarst lake (72°N, Russia) during an experiment spanning from April to August 2014 (Franz et al., 2018). In that study, the evaporation rate was near zero from April through mid-June (covering the ice-covered and break-up periods), subsequently averaging 2.5 mm d^{-1} and peaking at 6.0 mm d^{-1} during the ice-free period (July–September). These values are comparable to the evaporation rates observed over the ice-free Lake Zub/Priyadarshini in 2017–2018.

Evaporation from high-altitude lakes on the Qinghai-Tibetan Plateau (36°N, 3200–4700 m asl, China) has been extensively studied over the last few decades, with EC measurements spanning more than five years (Liu, 2016; Wang et al., 2019; Gan and Liu, 2020; Meng et al., 2020; Shi et al., 2024). Li et al. (2016) found that evaporation over the ice-free Lake Qinghai reaches up to 12 mm d^{-1} during storms, windy days (wind speed > 4 m s^{-1}) contribute up to 22 % of the annual lake evaporation, and a contribution is controlled more by wind speed than by the vapour pressure gradient or solar radiation. This aligns with our results, which indicate that wind is the primary driver of evaporation over the two glacial lakes. Although we did not measure radiation during our experiments, such data are routinely collected by instrumentation installed at the Maitri and Novo observatories, offering opportunities for future research into the lake surface energy balance.

Faucher et al. (2019) measure ice sublimation over the surface of the perennially frozen Lake Untersee (71° S, Antarctica) using ablation stakes over a two-year period, estimating total sublimation (evaporation) between 400 to 750 mm y^{-1}, which corresponds to a mean daily rate of 1.1–2.1 mm d^{-1}. These values are very close to the estimates obtained for the ice-covered Lake Glubokoe (2019–2020). Dugan et al. (2013) estimated lake ice ablation (sublimation) of 5–31 mm d^{-1} for lakes in Tailor Valley (77°S, Antarctica); however, the authors were unable to distinguish between between the contributions of surface melt and sublimation to total ablation during the summer. For winter, Dugan et al. (2013) reported sublimation values ranging from 0.2 mm d^{-1} to 0.7 mm d^{-1}, which are naturally much smaller than we observed for fully or partially ice-free lakes. Leppäranta et al. (2016) reported summertime ice sublimation of 0.7 mm d^{-1} for the lakes in the Vestfjella

Mountains, Droning Maud Land (73 °S, Antarctica), and ice thinning of 10–15 mm d^{-1} on a small pond on a nunatak during days when winds speeds exceeded 30 m s^{-1}. As no surface melt occurred during these high-wind events, the observed ice thinning was attributed to sublimation (Leppäranta et al., 2016). Although no EC observations were available for that site, our calculations using the bulk-aerodynamic method confirm that these thinning rates are physically plausible under such extreme wind speeds, provided the ice surface temperature is near 0 ºC and the air is very dry.

The bulk-aerodynamic method is highly sensitive to the moisture transfer coefficient (C_E) which is typically considered nearly constant at approximately $1.1\cdot10^{-3}$ over the ocean (Kantha and Clayson, 2000) and varies between $1.1\cdot10^{-3}$ and $2.4\cdot10^{-3}$ over natural and artificial lakes (Hicks, 1972; Guseva et al. 2022). Our results indicate that the moisture transfer coefficient (C_{E10N}) varying between $1.4\cdot10^{-3}$ for Lake Zub/Priyadarshini and $2.1\cdot10^{-3}$ for Lake Glubokoe. Using these site-specific values, the bulk-aerodynamic method underestimated lake evaporation by 6–8% with $s/\sigma < 0.80$ and RMSE of 0.6 mm d^{-1}. These metrics are within acceptable limits, supporting the use of this mass-transfer method to simulate hourly and daily lake evaporation rates in the Schirmacher Oasis. This aligns with conclusions from studies focusing on lake evaporation across the Qinghai-Tibetan Plateau (Wang et al., 2019).

The method used to calculate evaporation is particularly important for shallow Antarctic lakes, where water volume fluctuations are small throughout the summer season (Shevnina et al., 2021). Gopinath et al. (2020) demonstrated that summertime evaporation is a significant component of the water budget for shallow lakes in the Schirmacher Oasis, particularly Lake Zub/Priyadarshini. This lake serves as the freshwater supply for the Maitri research station, which hosts up to 25 people during the summer (Antarctic station catalogue, 2025). The planned opening of the new Maitri-II research station in 2032 — designed to accommodate up to 140 people, and it needs additional freshwater. Dhote et al. (2021) evaluated the components of water balance equation for Lake Zub/Priyadarshini, identifying precipitation, inlet river runoff, and wastewater return as positive contributors, while outlet river runoff, evaporation, and freshwater withdrawal act as negative components. The volume of Lake Zub/Priyadarshini decreased by 40.3 m^3 between January and February 2018, with a water balance equation residuals of 670.6 m^3 (Dhote et al., 2021). The lake evaporation estimate of 58.5 m^3 used by Dhote et al (2021) was calculated following Odrova (1979), and this method underestimated the lake evaporation by 72 %. This corresponds to an absolute difference of approximately 42.1 m^3, which accounts for roughly 6% of the water balance residuals. This discrepancy could be mitigated by employing the bulk-aerodynamic method with a neutral 10-m moisture transfer coefficient (C_{E10N}) equalling $2.1\cdot10^{-3}$. Meanwhile, the precipitation volume over Lake Zub/Priyadarshini during the same period was 5.3 m^3, representing 0.05% of the total lake volume. The remaining residual in the water balance is likely attributable to uncertainties in the methods used to evaluate inlet and outlet river runoff; our future research will specifically address these uncertainties.

The EC measurements remain rare on the lakes located north of 60° latitude. Ala-Könni et al. (2022) measured the evaporation over Lake Kuivajärvi (61°N, Finland) during the ice free period, and yielded the mean evaporation rate 1.5 – 2.5 mm d^{-1} during July – August; the evaporation up to 5 mm d^{-1} were observed in days with strong winds, or periods when dry and cold synoptic fronts pass. Blanken et al. (2000 and 2003) measured the evaporation over Great Slave Lake (62 °N, Canada) during the ice free period from June to September (1997, 1998, and 1999) when the evaporation rate reached 2.8 mm d^{-1}. The results imply that both (wind speed and vapor pressure gradient) control the evaporation over an ice free lake. Granger and Hedstrom (2011) estimated that 4–9 day-averaged evaporation rate reaches 3.2 – 3.9 mm d^{-1} during an ice free period for small lakes located next to Lake Great Slave. The northernmost EC measurements were obtained from a small Arctic thermokarst lake (72 °N, Russia) during an experiment spanning from April to August 2014 (Franz et al., 2018). The lake evaporation rate was estimated to be near zero from April through the mid June (covering the ice-covered and break-up periods), subsequently averaging 2.5 mm d^{-1} and peaking at 6 mm d^{-1} during the ice free period from July to September. These estimates of the lake evaporation are comparable with the evaporation over the ice-free Lake Zub/Priyadarshini measured with the EC technique (2017 – 2018).

Evaporation of the high-altitude lakes in the Qinghai-Tibetan Plateau (36°N, 3200 – 4700 m asl, China) has been extensively studied in last decades with the EC measurements spanning more than 5 years (Shi et al. 2024; Gan and Liu, 2020; Meng et al 2020; Wang et al., 2019; Li et al. 2016). Li et al. (2016) found that evaporation over the ice-free Lake Qinghai reaches up to 12 mm d^{-1} during storms, and windy days (wind speed > 4 m s^{-1}) contribute up to 22 % of the annual lake evaporation, and this contribution is comparable for the ice sublimation (23 %). Shi et al. (2024) conclude that evaporation over the ice-free Lake Qinghai is controlled by wind rather than by vapor pressure gradient or solar radiation. It is in accordance with our results shown that wind is the primary factor driving the evaporation over two lakes in Antarctica. We did not measure the radiation during the experiments, however, it is routinely measured with instrumentation installed at Maitri and Novo observatories. It opens opportunities for a new study on the lake surface energy balance.

Faucher et al. (2019) measure the ice sublimation over the surface of perennially frozen glacial Lake Untersee (71° S, Antarctica) with sticks during two years (), and estimate the sublimation (evaporation) between 400 to 750 mm year^{-1} which gives the mean daily rate 1.1–2.1 mm d^{-1}. It is very close to the estimates obtained for the ice-covered Lake Glubokoe (2019 – 2020). Dugan et al., (2013) estimate the lake ice ablation (sublimation) of 5–31 mm d^{-1} for the lake in Tailor Valley (77°S, Antarctica); the authors, however, did not have means to distinguish between the contributions of surface melt and sublimation to ablation during summer. For winter, Dugan et al. (2013) found sublimation values ranging from 0.2 to 0.7 mm d^{-1}, and these values are naturally much smaller than our results obtained for the fully or partially ice-free lakes.

Leppäranta et al. (2016) reported the summertime ice sublimation of 0.7 mm d^{-1} for the lakes in the Vestfjella mountains, Droning Maud Land (73°S, Antarctica), and the ice thinning of 10 – 15 mm d^{-1} on a small pond on top of a nunatak during days with the winds speeds exceeding 30 m s^{-1}. Because of no surface melt during days in such windy days, the ice thinning is likely attributed to sublimation (Leppäranta et al., 2016). No EC observations were available from the site but we checked that according to the bulk-aerodynamic method these values are indeed possible under such a wind speed, if the ice surface temperature is close to 0 °C and the air is very dry.

The bulk-aerodynamic method is sensitive to actual values of the transfer coefficient of moisture (C_E) which is typically considered almost constant with a value of approximately $1.1{\cdot}10^{-3}$ over the ocean (Kantha and Clayson, 2000) and varying between 1.1 and $2.4{\cdot}10^{-3}$ over the natural and artificial lakes (Hicks, 1972; Guseva et al. 2022). Our results showed that the transfer coefficient of moisture (C_{ENz} , z = 10 m) varying between $1.4{\cdot}10^{-3}$ and $2.1{\cdot}10^{-3}$ (Lake Zub/Priyadarshini and Lake Glubokoe, respectively). With these actual values, the bulk-aerodynamic method underestimated the evaporation by 6 – 8%, and got the scores $s/\sigma < 0.80$ and RMSE of 0.6 mm d^{-1}, which are acceptable to recommend this method to simulate the daily lake evaporation rate for two lakes in the Schirmacher oasis. It aligns to conclusions of the studies focusing on the evaporation over the lakes of Qinghai-Tibetan Plateau (Wang et al., 2019).

The method used in calculation of evaporation is important for the shallow coastal lakes whose volume changes very little over a summer (Shevnina and Kourzeneva, 2017). Gopinath et al. (2020) found that summertime evaporation is a significant component in the water budget of shallow lakes in the Schirmacher Oasis. Lake Zub/Priyadarshni supplies freshwater to the Maitri research station which is crewed with approximately 60 people at maximum during summers. A new Maitri-II research station is planned to open in 2032; expanding the investigation of Antarctica, it will accommodate up to 140 people (10 October 2025, **https://timesofindia.indiatimes.com/**). To plan the water supply/utilisation system of the stations, one should investigate (model) the water budget of Lake Zub/Priyadarshni. Dhote et al. (2021) evaluated the component of this lake water balance equation, namely the precipitation, inlet river runoff and wastewater return (as positive); and the outlet river runoff, evaporation and freshwater withdrawal (as negative).

The volume of Lake Zub/Priyadarshini is $1.03x10^{6}$ m^{3}, and in January – February 2018 it decreased by 40.3 m^{3}; the residuals of the water balance equation was 670.6 m3 (Dhote et al., 2021). The lake evaporation of 58.5 m^{3} was calculated following Odrova (1979), which underestimated the evaporation by72 % according to our results. In absolute values it corresponds to 42.1 m^{3} (58.5 multiplied by 0.72), which represents approximately 6% of the discrepancy of the water balance equation. It can be reduced by using the bulk-aerodynamic method with the neutral 10-m turbulent transfer coefficient of moisture (C_{ENz}, z = 10 m) equalling 2.1×10^{-3}. The volume of precipitation over the surface of Lake Zub/Priyadarshini was 5.3 m^{3} in January – February 2018, and it is 0.05% of the lake volume. The rest of discrepancy is likely contributed by methods used to evaluate the inlet/outlet river runoff.

Application of the traditional approaches to measure lake evaporation is limited by the difficulty of their maintenance and operation in Antarctica. Defining the actual values for the mass transfer and empirical coefficients requires detailed micrometeorological measurements on different heights which episodically done in Antarctica. The tracers-based approach may give an accurate estimate of lake evaporation (Fekete et al., 2006); it, also, requires regular water sampling followed by a unified programme. It, however, is relatively easy to organize on lakes located next to the human settlements.

6 Conclusions

We measured lake evaporation using the eddy covariance (EC) technique at two lakes in the Schirmacher Oasis (70°S), finding that summertime evaporation rates ranged from 0.3 to 5.0 mm d^{-1}. Depending on the presence of lake ice, mean evaporation varied from 1.6 ± 0.1 mm d^{-1} in the early stage of lake ice break-up (December) to 3.0 ± 0.2 mm d^{-1} during the ice-free period (January–February). Throughout the austral summer, the lakes remain warmer than the ambient air on most days. Variations in evaporation were primarily associated with changes in wind speed rather than fluctuations in the temperature gradient between the near-surface air and the lake surface water.

We further quantified the uncertainties of the bulk-aerodynamic method and five empirical formulas applied to estimate summertime evaporation over two lakes in coastal Antarctica. The bulk-aerodynamic method yielded the most accurate evaporation estimates (biases of 6–8 % for mean values) when the moisture transfer coefficient (C_{E10N}) was set to $1.4 \cdot 10^{-3}$ for Lake Zub/Priyadarshini and $2.1 \cdot 10^{-3}$ for Lake Glubokoe. This method demonstrated acceptable skill in estimating daily evaporation over both lakes during the ice break-up and open-water periods; consequently, it is recommended for hydrological (water balance) applications required for short-term operational decision-making. The selected empirical formulas underestimated daily evaporation over the lakes by 27–73%. However, with appropriate corrections, they can be used to estimate cumulative summertime evaporation for hydrological applications. These indirect methods require measurements of lake surface water temperature that can be estimated, for example, from satellites equipped with thermal sensors.

The application of traditional approaches for measuring water balance components, including lake evaporation, is limited by the logistical challenges of maintaining and operating equipment in Antarctica. Determining accurate values for mass-transfer and empirical coefficients requires detailed hydrological and micrometeorological measurements, which are currently conducted only occasionally in this region. While isotope tracer-based approach can provide an accurate estimate of lake evaporation, it also requires regular water sampling as part of a unified monitoring program. Nevertheless, this method is relatively easier to implement on lakes located in the vicinity of settlements visiting by tourists.

We measured the evaporation with the eddy-covariance technique on two lakes in the Schirmacher Oasis (70°S), and estimated the summertime lake evaporation varied from 0.3 to 5.0 mm d^{-1}. Depending on the presence of lake ice, the average evaporation varied from 1.6 ± 0.2 mm d^{-1} in the early stage of lake ice break-up (December) to 3.0 ± 0.3 mm d^{-1} for the lake ice-free period (January – February). During the austral summer, the lakes are warmer than the ambient air on most days. The changes in evaporation were associated with changes in wind speed rather than changes in difference between the near-surface air temperature and lake surface water temperature.

We further quantified uncertainties in the bulk-aerodynamic method and five empirical formulas have been applied in estimations of summertime evaporation over two lakes in coastal Antarctica. The bulk aerodynamic method yielded the most accurate estimates of evaporation (biases of 6 – 8 % for the mean values) when the moisture transfer coefficient (C_{ENz}, z = 10 m) was set to $1.4 \cdot 10^{-3}$ and $2.1 \cdot 10^{-3}$ for Lake Zub/Priyadarshini and Lake Glubokoe, respectively. This method showed an

~~acceptable skill in estimation of the daily evaporation over both lakes during the ice break-up and open water periods. Hence, the method can be recommended for hydrological (lake water balance) applications required for operational (short term) decision making. The selected empirical formulas underestimated the daily evaporation over the lakes by 27–73%. With the correction, however, they can be applied to estimate the cumulative summertime evaporation, which is needed for the hydrological applications required for decisions on sites' maintenance and investment. These indirect methods need the measurements of lake surface water temperature.~~

Code availability. The code is available on GitHub~~at the Github~~. The code used to generate Figures 3–~~for the figures 3, 4, 6, 7, 8 and~~ 9 was developed with the assistance of GitHub~~written using suggestions given by the AI Github~~ Copilot.

Data availability. The dataset is available at https://doi.org/10.5281/zenodo.14823402.

Interactive computing environment. Pycharm at Ubuntu (Noble Nombat).

Supplements. The evaporation estimated after the EC (direct) and indirect methods are given in ECH_ZB/GL.csv and BA_daily_ZB/GL.csv.

Author contribution. ES designed and conducted the field experiments, calculated evaporation using empirical equations, and performed the uncertainty and skill score analyses. TV and TN estimated evaporation using the bulk-aerodynamic method, and analysed the meteorological conditions during the experimental periods. MP designed and analysed the EC measurements from the field experiments. All authors contributed to the writing of the manuscript. This manuscript was proofread and edited for English language proficiency, flow, and clarity using the Gemini AI system. Final proofreading was made by the authors.

~~**Author contribution.** ES designed and ran the field experiments as well as calculated the evaporation applying the empirical equations, their uncertainties, and skill scores. TV estimated the evaporation with the bulk-aerodynamic method. MP designed and analyzed the EC measurements in the field experiments. TN analyzed synoptic situation and weather during the experiments. All authors contributed to writing of the manuscript.~~

Competing interests. The corresponding author declares that there are no competing interests for any of the authors~~contact author has declared that none of the authors has any competing interests~~.

Disclaimer. Publisher's note: Copernicus Publications remains neutral with regard to jurisdictional claims in published maps and institutional affiliations.

Acknowledgments. This research was supported by the European Union's Horizon 2020 research and innovation framework program under Grant Agreement No. 101003590 (PolarRES project) and the Research Council of Finland under Grant 364657 (CAAC project). The authors thank the European Commission and Fundação para Ciência e Tecnologia (FCT) for funding in the frame of the collaborative international consortium INTERLAYER financed under the 2022 Joint call of the European Partnership 101060874 — Water4All (Water4All-2022-00261). We thank all participants of the Annual Meeting of the European Meteorological Society (EMS) (1–7 September 2024, Barcelona, Spain) and the 7th Workshop on Parameterization of Lakes in Numerical Weather Prediction and Climate Modeling (20–22 November 2024, Milan, Italy) for their valuable questions and discussions. We thank Dmitrii Emelyanov, Ivan Kolesnikov, Alexey Tyltin and Pankaj Ramji

Dhote, who were involved in instrumentation maintenance during the field campaigns. We thank Adriaan J. (Ryan) Teuling and the four reviewers, whose comments helped to improve the manuscript.

Acknowledgments. This research has been supported by the European Union's Horizon 2020 research and innovation framework program under Grant Agreement no. 101003590 (PolarRES project). We thank participants of the Annual Meeting – European meteorological society, EMS (1-7 September 2024, Barselona, Spain) and 7th workshop on parametrization of lakes in numerical weather prediction and climate modeling (20-22 November 2024, Milan, Italy) for questions and discussions during the conferences. We thank Dmitrii Emelyanov, Ivan Kolesnikov and Pankaj Ramji Dhote who were involved in the instrumentation maintenance during the field campaigns. We thanks four reviewers whose comments helped to improve the manuscript.

References

Abtew W., Melesse A.: Evaporation and Evapotranspiration Estimation Methods. In: Evaporation and Evapotranspiration. Springer, Dordrecht, doi: 10.1007/978-94-007-4737-1_6, 2013.

Ala-Könni, J., Kohonen, K.-M., Leppäranta, M., Mammarella, I.: Validation of turbulent heat transfer models against eddy covariance flux measurements over a seasonally ice-covered lake, Geosci. Model Dev., 15, 4739–4755, https://doi.org/10.5194/gmd-15-4739-2022, 2022.

Andreas E. L.: A theory for the scalar roughness and the scalar transfer coefficients over snow and sea ice. CRREL Report 86-9, 26 pp., 1986.

Andersen, D., Sumner, D., Hawes, I., Webster-Brown, J., McKay, C.: Discovery of large conical stromatolites in Lake Untersee, Antarctica. Geobiology 9, 280–293, 2011.

Antarctic station cataloguecatalog: Council of Managers of National Antarctic Programs (COMNAP), 2015.

Arya, S.P.: Introduction to Micrometeorology. Academic Press, 307 pp., 1988.

Arthur, J.F., Stokes, C.R., Jamieson, S.S.R., Carr, J. R., Leeson, A. A. Verjans V.: Large interannual variability in supraglacial lakes around East Antarctica. Nat Commun 13, 1711. https://doi.org/10.1038/s41467-022-29385-3, 2022.

Asthana, R., Shrivastava, P.K., Srivastava, H.B., Swain, A.K., Beg, M.J., Dharwadkar, A.: Role of lithology, weathering and precipitation on water chemistry of lakes from Larsemann Hills and Schirmacher Oasis of East Antarctica, Adv Polar Sci, 2019, 30(1): 35-51, doi: 10.13679/j.advps.2019.1.00035, 2019.

Banwell A.F., MacAyeal D.R., Sergienko O.V.: Breakup of the Larsen B ice shelf triggered by chain reaction drainage of supraglacial lakes. Geophys Res Lett. 40(22):5872–5876, doi: 10.1002/2013GL057694, 2013.

Bastmeijer, K., Shibata A., Steinhage, Ferrada, L.V., Bloom E.T.: Regulating Antarctic Tourism: The Challenge of Consensus-Based Decision Making, American Journal of International Law, 117(4), pp. 651–676. doi: 10.1017/ajil.2023.34, 2023.

Bellagamba, A. W., Berkelhammer, M., Winslow, L., Doran, P. T.,Myers, -K. F., -Devlin, S., Hawes I.: -The magnitude and climate sensitivity of isotopic fractionation from ablation of Antarctic Dry Valley lakes, Arctic, Antarctic, and Alpine Research, 53:1, 352-371, doi ~~DOI~~: 10.1080/15230430.2021.2001899, 2021.

Blanken, P. D., Rouse, W. R., Culf, A. D., Spence, C., Boudreau, L. D., Jasper, J. N., Kochtubajda, B., Schertzer, W. M., Marsh, P., ~~and~~ Verseghy, D.: Eddy Covariance Measurements of Evaporation from Great Slave Lake, Northwest Territories, Canada, Water Resources Research, 36, 1069–1077, https://doi.org/10.1029/1999WR900338, 2000.

Blanken, P. D., Rouse, W. R., Schertzer, W. M. Enhancement of Evaporation from a Large Northern Lake by the Entrainment of Warm, Dry Air. Journal of Hydrometeorology, 4(4), 680-693. https://doi.org/10.1175/1525-7541(2003)004<0680:EOEFAL>2.0.CO;2, 2003.

Blanken, P. D., Spence, C., Hedstrom, N., ~~and~~ Lenters, J. D.: Evaporation from Lake Superior: 1. Physical Controls and Processes, Journal of Great Lakes Research, 37, 707–716, https://doi.org/10.1016/j.jglr.2011.08.009, 2011.

Bliss, A.K., Cuffey, K.M., Kavanaugh, J.L.: Sublimation and surface energy budget of Taylor Glacier, Antarctica, Journal of Glaciology, 57(204), pp. 684–696. doi:10.3189/002214311797409767, 2011.

Borghini, F., Colacevich, A., Loiselle, S.A. et al. 2013: Short-term dynamics of physico-chemical and biological features in a shallow, evaporative antarctic lake. Polar Biol 36, 1147–1160. https://doi.org/10.1007/s00300-013-1336-2, 2013.

Brutsaert, W., : Evaporation into the atmosphere - theory, history and applications, Dordrecht, Holland: D Reidel Publishing Company, Dordrecht, Holland, 299 pp., 1982

Burba G. Eddy Covariance Method for Scientific, Industrial, Agricultural, and Regulatory Applications: A Field Book on Measuring Ecosystem Gas Exchange and Areal Emission Rates. LI-COR Biosciences, Lincoln, NE, USA, 331 p., 2013.

Businger, J. A., Wyngaard, J. C., Izumi, Y., and Bradley, E. F.: Flux-Profile Relationships in the Atmospheric Surface Layer, J. Atmos. Sci., 28, 181–189, https://doi.org/10.1175/1520-0469(1971)028<0181:FPRITA>2.0.CO;2, 1971.

Corr, D., Leeson, A., McMillan, M., Zhang, C., and Barnes, T.: An inventory of supraglacial lakes and channels across the West Antarctic Ice Sheet, Earth Syst. Sci. Data, 14, 209–228, https://doi.org/10.5194/essd-14-209-2022, 2022.

~~Chebotarev, A. I.: Hydrology, Gidrometizdat, Leningrad, 544 pp., 1975 (in Russian).~~

Clow, G. D., -McKay, C. P.,Simmons, G. M., Wharton, R. A.: Climatological observations- and predicted sublimation rates at Lake Hoare, Antarctica. J. Climate, 1, 715–728, https://doi.org/10.1175/1520-0442(1988)001<0715:COAPSR>2.0.CO;2, 1988.

Dirscherl, M. C., Dietz, A. J., Kuenzer, C.: Seasonal evolution of Antarctic supraglacial lakes in 2015–2021 and links to environmental controls, The Cryosphere, 15, 5205–5226, https://doi.org/10.5194/tc-15-5205-2021, 2021.

Doorenbos, J., Pruitt, W.O.: Crop water requirements, FAO Irrigation and Drainage Paper No. 24 FAO Rome, 179pp., 1975.

Dhote, P. R., Thakur, P. K., Shevnina, E., Kaushik, S., Verma, A., Ray, Y., Aggarwal, S. P.: Meteorological parameters and water balance components of Priyadarshini Lake at the Schirmacher Oasis, East Antarctica, Polar Sci., 30, 100763, https://doi.org/10.1016/J.POLAR.2021.100763, 2021.

Dugan, H.A., Obryk, M.K., Doran, P.T.: Lake ice ablation rates from permanently ice-covered Antarctic lakes’, Journal of Glaciology, 59(215), pp. 491–498. doi:10.3189/2013JoG12J080, 2013.

Gan, G., Liu, Y.: Heat storage effect on evaporation estimates of China's largest freshwater lake. Journal of Geophysical Research: Atmospheres, 125, e2019JD032334. https://doi.org/10.1029/2019JD032334, 2020.

Gerrish, L., Fretwell, P., Cooper, P.: High resolution Antarctic lakes dataset (7.3) [Data set]. UK Polar Data Centre, Natural Environment Research Council, UK Research & Innovation. https://doi.org/10.5285/6a27ab9e-1258-49b1-bd2c-fcbed310ab45, 2020.

Gilson, G.F., Jiskoot, H., Cassano, J.J., Gultepe, I., James T.D.: The Thermodynamic Structure of Arctic Coastal Fog Occurring During the Melt Season over East Greenland. Boundary-Layer Meteorol 168, 443–467, https://doi.org/10.1007/s10546-018-0357-3, 2018.

Gopinath, G., Resmi, T. S., Praveenbabu, M., Pragath, M., Sunil, P. S., Rawat, S.: Isotope hydrochemistry of the lakes in Schirmacher Oasis, East Antarctica. Indian Journal of Geo Marine Sciences Vol. 49 (6), 947-953, 2020.

~~Govil, P., Mazumder A., Asthana R., Tiwari A., Mishra R.: Holocene climate variability from the lake sediment core in Schirmacher Oasis region, East Antarctica: Multiproxy approach, Quaternary International, doi:1016/j.quaint.2016.09.032, 2016.~~

Granger, R. J. and Hedstrom, N.: Modelling hourly rates of evaporation from small lakes, Hydrol. Earth Syst. Sci., 15, 267–277, https://doi.org/10.5194/hess-15-267-2011, 2011.

~~Grazioli, J., Madeleine, J.-B., Gallée, H., Forbes, R. M., Genthon, C., Krinner, G., Berne, A.: Katabatic winds diminish precipitation contribution to the Antarctic ice mass balance, P. Natl. Acad. Sci. USA, 114, 10858–10863, https://doi.org/10.1073/pnas.1707633114, 2017.~~

Guest, P. S.: Inside katabatic winds over the Terra Nova Bay polynya: 2. Dynamic and thermodynamic analyses, J. Geophys. Res.-Atmos., 126, e2021JD034904, https://doi.org/10.1029/2021JD034904, 2021.

Guseva, S., Armani, F., Desai, A. R., Dias, N. L., Friborg, T., Iwata, H., et al.: Bulk transfer coefficients estimated from eddy-covariance measurements over lakes and reservoirs. Journal of Geophysical Research: Atmospheres, 128, e2022JD037219. https://doi.org/10.1029/2022JD037219, 2023.

Faucher, B., Lacelle, D., Fisher, D., Andersen, D., McKay, C.: Energy and water mass balance of Lake Untersee and its perennial ice cover, East Antarctica. Antarctic Science, 31(5), 271-285. doi:10.1017/S0954102019000270, 2019.

Fedorovich, E. E., Golosov, S. D., Kreiman, K. D., Mironov, D. V., Shabalova, M. V. et al: Modeling air-lake interaction. In Physical Background (ed. S. S. Zilitinkevich) Springer Verlag, Berlin, 130 pp., 1991.

Finch, J. W., Hall, R. L.: Estimation of open water evaporation: A Review of methods, R&D Technical Report W6-043/TR. Environment Agency, Bristol, 155 pp., 2001.

~~Fekete, B. M., Gibson, J. J., Aggarwal, P., and Vörösmarty, C. J.: Application of isotope tracers in continental scale hydrological modeling, J. Hydrol., 330, 444–456, 2006.~~

Finch, J. W., Calver, A.: Methods for the quantification of evaporation from lakes, Prepared for the World Meteorological Organization's Commission for Hydrology, Oxfordshire, UK, 41 pp., 2008.

Finch, J. W., Hall, R. L.: Estimation of open water evaporation: A Review of methods, R&D Technical Report W6-043/TR. Environment Agency, Bristol, 155 pp., 2001.

Franz, D., Mammarella, I., Boike, J., Kirillin, G., Vesala, T., Bornemann, N., et al.: Lake-atmosphere heat flux dynamics of a thermokarst lake in arctic Siberia. Journal of Geophysical Research: Atmospheres, 123, 5222– 5239. https://doi.org/10.1029/2017JD027751., 2018.

Heikinheimo, M., Kangas, M., Tourula, T., Venäläinen, A., Tattari, S.: Momentum and heat fluxes over lakes Tämnaren and Råksjö determined by the bulk-aerodynamic and eddy-correlation methods, Agric. Forest Meteorol., 98–99, 521–534, https://doi.org/10.1016/S0168-1923(99)00121-5, 1999.

Hicks, B.B.: Some evaluations of drag and bulk transfer coefficients over water bodies of different sizes. Boundary-Layer Meteorol 3, 201–213. https://doi.org/10.1007/BF02033919, 1972.

Hoeltgebaum, L. E. B., Diniz, A. L., and Dias, N. L. C.: Intercomparação de sensores de temperatura e umidade relativa para uso em campanha micrometeorológica, 2020, Ci. e Nat., Santa Maria v.42, Special Edition: Micrometeorologia, e18, https://doi.org/10.5902/2179460X46565, 2020. (In (in Portuguese).

Holtslag, A. A. M., De Bruin, H. A. R.: Applied Modeling of the Nighttime Surface Energy Balance over Land, Journal of Applied Meteorology, Vol. 27, No. 6, , 689-704. http://dx.doi.org/10.1175/1520-0450(1988)027<0689:AMOTNS>2.0.CO;2, 1988.

Kantha, L.H., Clayson, C.A.: Numerical Models of Oceans and Oceanic Processes, Academic Press, California, USA, 2000.

Kaup, E.: The salinity and temperature of the lakes of the Larsemann Hills, East Antarctica. *Antarctic Science*, 13(1), pp. 31–36, 2001.

Kaup, E.: Development of anthropogenic eutrophication in lakes of the Schirmacher Oasis, Antarctica. Verh. Internat. Verein. Limnol. 29, 678-682, 2005.

Keskitalo, J., Leppäranta, M., Arvola, L. First records of primary producers of epiglacial and supraglacial lakes in western Dronning Maud Land, Antarctica. Polar Biol 36, 1441–1450, https://doi.org/10.1007/s00300-013-1362-0, , 2013.

Khare, N., Chaturvedi, S. K., Saraswat, R., Srivastava, R., Raina R., Wanganeo, A.: Some morphometric characteristics of Priyadarshini water body at Schirmacher Oasis, Central Dronning Maud Land, Antarctica with special reference to its bathymetry. Indian Journal of Marine Sciences, 37(4), 435-438, 2008.

Kljun, N., Calanca, P., Rotach, M. W., Schmid, H. P.: A Simple Parameterisation for Flux Footprint Predictions, Bound.-Lay. Meteorol., 112, 503–523, https://doi.org/10.1023/B:BOUN.0000030653.71031.96, 2004.

Keijman, J.Q.: The estimation of the energy balance of a lake from simple weather data. Boundary-Layer Meteorol, 1974, 7: 399, doi: 10.1007/BF00240841, 1974.

Kuznetsova M.R., Priakhina G.V., Grigoreva S.D., Kiniabaeva E.R. Formation factors of surface inflow to Antarctic lakes of the Larsemann Hills oasis. Problemy Arktiki i Antarktiki. Arctic and Antarctic Research. 2021, 67 (3): 293–309 [In Russian]. https://doi.org/10.30758/0555-2648-2021-67-3-293-309, 2021. (In Russian).

Lan, T., Li, T., Zhang, H., Wu, J., Chen, Y. D., Xu, C.-Y.: Exploring the potential processes controlling changes in precipitation–runoff relationships in non-stationary environments, Hydrol. Earth Syst. Sci., 29, 903–924, https://doi.org/10.5194/hess-29-903-2025, 2025.

Launiainen, J., Vihma, T.: Derivation of turbulent surface fluxes – An iterative flux-profile method allowing arbitrary observing heights, Environ. Softw., 5, 113–114, https://doi.org/10.1016/0266-9838(90)90021-W, 1990.

Loopman, A., Kaup, E., Klokov, V., Simonov, I., Haendel, D.: The bathymetry of some lakes of the Antarctic oases Schirmacher and Untersee, in Limnological Studies in Queen Maud Land (East Antarctic), Ed. by J. Martin (Valgus, Tallinn), 6–14, 1988.

Leppäranta, M., Lindgren, E., Arvola, L. Heat balance of supraglacial lakes in the western Dronning Maud Land. Annals of Glaciology, 57(72):39-46. doi:10.1017/aog.2016.12, 2016.

Leppäranta, M., Luttinen, A., Arvola, L.: Physics and geochemistry of lakes in Vestfjella, Dronning Maud Land, Antarctic Science, 32(1), pp. 29–42. doi:10.1017/S0954102019000555, 2020.

Li, X. Y., Ma, Y. J., Huang, Y. M., Hu, X., Wu, X. C., Wang, P., Li, G.Y. , Zhang, Z.S., Wu, H.W., –Jiang, Z.Y., -Cui, B.L.,- Liu, L.: Evaporation and surface energy budget over the largest high-altitude saline lake on the Qinghai-Tibet Plateau. Journal of Geophysical Research: Atmospheres, 121, 10,470–10,485. https://doi.org/10.1002/2016JD025027, 2016.

Liu, X.: Accuracy of methods for simulating daily water surface evaporation evaluated by the eddy covariance measurement at boreal flux sites, J. Hydrol., 616, 128776, doi: https://doi.org/10.1016/j.jhydrol.2022.128776, 2023.

Marsh, P., and Verseghy, D.: Eddy covariance measurements of evaporation from great slave Lake, northwest territories, Canada. Water Resources Research, 36(4), 1069–1077, https://doi.org/10.1029/1999WR900338, 2000.

Meng X, Liu H, Du Q, Xu L, Liu Y. Evaluation of the Performance of Different Methods for Estimating Evaporation over a Highland Open Freshwater Lake in Mountainous Area. Water. 12(12):3491. https://doi.org/10.3390/w12123491, 2020.

Moriasi, D. N., Arnold, J. G., Van Liew, M. W., Bingner, R. L., Harmel, R. D., and Veith, T. L.: Model evaluation guidelines for systematic quantification of accuracy in watershed simulations, T. ASABE, 50, 885–900, https://doi.org/10.13031/2013.23153, 2007.

Moore, R.D.: On use of bulk aerodynamic formulae over melting snow, Nordic Hydrology, 1983, 193-206, 1983.

Morton, F.I.: Studies in evaporation and their lessons for the environmental sciences Can Water Resour J, 15 (3) , pp. 261-286, 10.4296/cwrj1503261, 1990.

Naakka, T., Nygård, T., Vihma, T.: Air moisture climatology and related physical processes in the Antarctic on the basis of ERA-5 reanalysis, J. Climate, 34, 4463–4480, https://doi.org/10.1175/JCLI-D-20-0798.1, 2021.

Nygård, T., Valkonen T., Vihma, T. : Antarctic low tropospheric humidity inversions: 10-yr climatology. J. Climate, 26, 5205–5219, https://doi.org/10.1175/JCLI-D-12-00446.1, 2013

Nordbo, A., ~~S.~~ Launiainen, S.,~~I.~~ Mammarella, I.,~~M.~~ Leppäranta, M.,~~J.~~ Huotari, J.,~~A.~~ Ojala, A., Vesala, T.~~and T. Vesala~~: Long-term energy flux measurements and energy balance over a small boreal lake using eddy covariance technique, J. Geophys. Res., 116, D02119, doi:10.1029/2010JD014542, 2011.

Odrova, T. V. Hydrophysics of land water bodies, Hydrometeizdat, Leningrad, pp. 1–312, 1979. (in Russian).

Penman, H. L.: Natural evaporation from open water, bare soil and grass, P. Roy. Soc. Lond. A, 194, 120–145, https://doi.org/10.1098/rspa.1948.0037, 1948.

Phartiyal, B., Sharma, A., Bera, S.K.: Glacial lakes and geomorphological evolution of Schirmacher Oasis, East Antarctica during Quaternary. Quaternary International 23, 128–136, doi:10.1016/j.quaint.2010.11.025, 2011.

Popov, E. G.: Hydrological forecasts, Leningrad, Gidrometeoizdat, 257 pp., 1979 (in Russian).

Potes M., Salgado R., Costa M.J., Morais M., Bortoli D., Kostadinov I. and Mammarella I.: Lake–atmosphere interactions at Alqueva reservoir: a case study in the summer of 2014, Tellus A: Dynamic Meteorology and Oceanography, 69:1, doi: 10.1080/16000870.2016.1272787, 2017.

Bormann P, ~~Richter, W., Bormann, P., 1995. Hydrology //Bormann P,~~ Fritzsche D.: The Schirmacher Oasis, Queen Maud Land, East Antarctica, and its surroundings. Justus Perthes Verlag, Gotha, 259-319. 1995

Rignot, E., Casassa, G., Gogineni, P., Krabill, W., Rivera, A., Thomas, R.: Accelerated ice discharge from the Antarctic Peninsula following the collapse of Larsen B ice shelf. Geophys Res Lett. 31(18):L18401., doi: 10.1029/2004GL020697, 2004.

Rodrigues, C. M., Moreira, M., Guimarães, R. C., Potes, M.: Reservoir evaporation in a Mediterranean climate: comparing direct methods in Alqueva Reservoir, Portugal, Hydrol. Earth Syst. Sci., 24, 5973–5984, https://doi.org/10.5194/hess-24-5973-2020, 2020.

Rothschild, L., Mancinelli, R.: Life in extreme environments. Nature 409, 1092–1101. https://doi.org/10.1038/35059215, 2001.

Rozhdestvensky A.V., Chebotarev A.I.: Statistical methods in hydrology. Leningrad, Gidrometeoizdat. 1974. (In~~in~~ Russian).

Sengupta, S.: Structural and petrographical evolution of basement rocks in the Schirmacher hills, Queens Maud land, east Antarctica. In: Thompson, M.R.A., Crame, J.A., Thompson, J.W. (Eds.), Geological Evolution of Antarctica. Cambridge University Press, Cambridge, pp. 95-97, 1991.

Simonov, I. M., ~~and~~ Fedotov, V. I.: Ozera oasisa Schimachera [Lakes of the Schirmacher oasis], Informazioni bulletin Sovetskoy Antarcticheskoy Expedicii, 47, 19–23, 1964. (In Russian).

Sharov, A.N., ~~and~~ Tolstikov, A.V.: Hydrological and biological regimes of lakes of East Antarctica. Ecosystem Transformation 3 (3), 3–11, https://doi.org/10.23859/estr-200318, 2020.

Singh, V.P., Xu, C.Y.: ~~–~~Evaluation and generalization of 13 mass-transfer equations for determining free water evaporation. Hydrol. Process., 11: 311-323. https://doi.org/10.1002/(SICI)1099-1085(19970315)11:3<311::AID-HYP446>3.0.CO;2-Y, 1997.

Shi, F., Li, X., Zhao, S., Ma, Y., Wei, J., Liao, Q., and Chen, D.: Evaporation and sublimation measurement and modeling of an alpine saline lake influenced by freeze–thaw on the Qinghai–Tibet Plateau, Hydrol. Earth Syst. Sci., 28, 163–178, https://doi.org/10.5194/hess-28-163-2024 , 2024.

Shen, X.-Y., Ke, C.-Q., Li, H.-L., Cai, Y., Xiao, Y., Li, M.-M.: Evolution of supraglacial lakes over the pan-Antarctic ice sheet between 2014–2022: Assessment and the control factors, - Advances in Climate Change Research, 1674-9278, https://doi.org/10.1016/j.accre.2025.02.005, 2025.

Shevnina, E., Kourzeneva, E.: Thermal regime and components of water balance of lakes in Antarctica at the Fildes peninsula and the Larsemann Hills. Tellus A: Dynamic Meteorology and Oceanography, 69(1), doi:10.1080/16000870.2017, 2017.

Shevnina, E., Kourzeneva, E., Dvornikov, Y., Fedorova, I.: Retention time of lakes in the Larsemann Hills oasis, East Antarctica, The Cryosphere, 15, 2667–2682, https://doi.org/10.5194/tc-15-2667-2021, 2021.

Shevnina, E., Potes, M., Vihma, T., Naakka, T., Dhote, P. R., and Thakur, P. K.: Evaporation over a glacial lake in Antarctica, The Cryosphere, 16, 3101–3121, https://doi.org/10.5194/tc-16-3101-2022, 2022.

Shuttleworth, W. J.: Evaporation, in: Handbook of Hydrology, edited by: Maidment, D. R., McGraw-Hill, New York, 4.1–4.53,1993.

Sokratova, I. N.: Hydrological investigations in the Antarctic oases, Russ. Meteorol. Hydrol., 36, 207, https://doi.org/10.3103/S1068373911030083, 2011 (in Russian).

Spank, U., Koschorreck, M., Aurich, P., Sanchez Higuera, A. M., Raabe, A., Holstein, P. , Bernhofer, C., Mauder, M.: Rethinking evaporation measurement and modelling from inland waters − A discussion of the challenges to determine the actual values on the example of a shallow lowland reservoir, Journal of Hydrology, Volume 651, 132530, https://doi.org/10.1016/j.jhydrol.2024.132530, 2025.

Spence, C., Rouse, W. R., Worth Rouse, D., Oswald, C.: Worth, and C. Oswald. Energy budget processes of a small northern lake. Journal of Hydrometeorology 4: 694–701. 2003.

Spence C., Hedstrom H.: Attributes of Lake Okanagan evaporation and development of a mass transfer model for water management purposes, Canadian Water Resources Journal / Revue canadienne des ressources hydriques, DOI: 10.1080/07011784.2015.1046140, 2015.

Stanhill, G.: Is the class A evaporation pan still the most practical and accurate meteorological method for determining irrigation water requirements? Agric. Forest Meteorol. 112 (3–4), 233–236, 2002.

Stannard, D. I., Rosenberry, D. O.: A comparison of short-term measurements of lake evaporation using eddy correlation and energy budget methods. Journal of Hydrology, 122(1-4), 15–22. https://doi.org/10.1016/0022-1694(91)90168-H, 1991.

Stewart, R. B., Rouse, W. R.: A simple method for determining the evaporation from shallow lakes and ponds, Water Resour. Res., 12(4), 623–628, doi:10.1029/WR012i004p00623, 1976.

Stokes, C. R., Sanderson, J. E., Miles, B. W. J., Jamieson, S. S. R., Leeson, A. A.: Widespread distribution of supraglacial lakes around the margin of the East Antarctic Ice Sheet, Sci. Rep.-UK, 9, 13823, https://doi.org/10.1038/s41598-019-50343-5, 2019.

Stull, R.: Practical Meteorology: An Algebra-based Survey of Atmospheric Science ~~—~~version 1.02b, Univ. of British Columbia, 940 pp., 2017.

Su, D., Wen, L., Gao, X., Leppäranta, M., Song, X., Shi, Q., Kirillin, G.: Effects of the largest lake of the Tibetan plateau on the regional climate. J Geophys Res: Atmos 125, e2020JD033396, 2020.

Tanny, J., Cohen, S., Assouline S., Lange, F., Grava, A., Berger D., Teltch, B., Parlange, M.B.: Evaporation from a small water reservoir: Direct measurements and estimates. Journal of Hydrology, 351, 218– 229, 2008.

~~Tran, B. N., van der Kwast, J., Seyoum, S., Uijlenhoet, R., Jewitt, G., Mul, M.: Uncertainty assessment of satellite remote-sensing-based evapotranspiration estimates: a systematic review of methods and gaps, Hydrol. Earth Syst. Sci., 27, 4505–4528, https://doi.org/10.5194/hess-27-4505-2023, 2023.~~

Vickers, D., Mahrt, L.: Quality control and flux sampling problems for tower and aircraft data, J. Atmos. Ocean. Tech., 14, 512–526, https://doi.org/10.1175/1520-0426(1997)014<0512:QCAFSP>2.0.CO;2, 1997.

Wang, B., Ma, Y., Ma, W., Su, B., Dong, X.: Evaluation of ten methods for estimating evaporation in a small high-elevation lake on the Tibetan Plateau. Theoretical and Applied Climatology, 136(3), 1033-1045, 2019.

Wang, B., Ma, Y., Su, Z., Wang, Y., Ma, W.: Quantifying the evaporation amounts of 75 high-elevation large dimictic lakes on the Tibetan plateau. Science Advances, 6(26), eaay8558, 2020.

Yang, Z., Bai, P. Evaporation from snow surface: A multi-model evaluation with the FLUXNET 2015 dataset, Journal of Hydrology, 621, ~~Volume 621,~~ 129587, https://doi.org/10.1016/j.jhydrol.2023.129587, 2023.